

SCOUR BY SUBMERGED CIRCULAR IMPINGING JETS AND PROTECTION USING GEOTEXTILES

*A Thesis Submitted
in Partial Fulfilment of the Requirements
for the Degree of*

MASTER OF TECHNOLOGY

by

MANOJ TIWARI

to the

**DEPARTMENT OF CIVIL ENGINEERING
INDIAN INSTITUTE OF TECHNOLOGY KANPUR
DECEMBER, 1989**

C E R T I F I C A T E

This is to certify that this thesis entitled, "Scour by Submerged Circular Impinging Jets and its Protection Using Geotextiles", by Mr. Manoj Tiwari, for the award of the degree of Master of Technology, has been carried out under my guidance and that his work has not been submitted elsewhere for the award of any degree.

(Signature)

(Dr. T. Gangadharaiiah)
Professor

Department of Civil Engineering
Indian Institute of Technology, Kanpur

December, 1989.

- 4 APR 1990

CENTRAL LIBRARY
I I T KANPUR

Acc No. A10787

CE-1989-M-TIW-SCC

ACKNOWLEDGEMENT

I express my sincere gratitude to Prof. T.Gangadharaiiah for initiating me to proceed with this Thesis. I am extremely grateful to him for his constant motivation and expert guidance. It was for his inspiration and critical comments that this research work could take this shape. I also thank him for introducing me to the fundamentals of mechanism of sediment transportation during my course work.

I also thank all the faculty members who helped me update my knowledge through the courses they offered.

I am highly thankful to Prof. M.S.Madhav for helping me during my Thesis work.

I am grateful to the Laboratory staff for the help rendered by them during my stay here.

I take great pride in acknowledging all my friends who made my stay a memorable one. I am specially grateful to Gautam Roy, Muzzammil Saheb, Atul Namdev for the encouragement and help given by them.

I am also thankful to Mr. K.P. Gupta for excellent typing.

ABSTRACT

An experimental study is conducted on scour caused by submerged circular impinging water jet on the beds of cohesionless sediment of median diameter 2 mm and 0.17 mm. An attempt is also made to study the performance of geotextiles as a scour protection device. The characteristic features of scoured bed in the asymptotic state have been analysed. It is observed that initially the dynamic scour depth increases with time in logarithmic trend then it departs from logarithmic trend and attains a limiting value. The dynamic scour depth in asymptotic state, when the jet is on, static scour depth after stopping the jet, are found to be function of densimetric Froude number F_j , height of impingement and square root of the area of the nozzle A_j as $F_j/(H/\sqrt{A_j})$. Experimental data available in literature for circular wall jet of water on sand of median diameter 3, 2 and 1 mm and solid circular jet of air on sand ($D = 0.26$ mm), polystyrene ($D = 1.4$ mm) also agree with this functional form. Radius of scour hole in asymptotic state, is found to be function of $F_j/P_1(H/\sqrt{A_j})$, where P_1 takes into account the effect of viscosity on fall velocity. It is found that geotextile can prevent scouring very effectively provided that it is anchored properly and placed at $2 d_j$ and $4 d_j$ below or bed level.

C O N T E N T S

Sl.No.	Particulars	Page No.
1	Certificate	i
2	Acknowledgement	ii
3	Abstract	iii
4	Contents	iv
5	List of Figures	vi
6	List of Symbols	vii
7	List of Tables	viii
8	Chapter 1 INTRODUCTION	1
9	Chapter 2 LITERATURE REVIEW	4
	2.1 Diffusion of Submerged Jets	4
	2.2 Scouring Characteristics	5
	2.3 Scour Control	9
10	Chapter 3 GEOTEXTILES AS AN EROSION CONTROL DEVICE	
	3.1 Geotextile in Perspective	12
	3.1.1 Basic Geotextile Functions	12
	3.2 Types of Geotextile	13
	3.2.1 Raw materials	13
	3.2.2 Woven Geotextile	14
	3.2.3 Non-woven Geotextile	14
	3.3 Erosion Control	15
	3.3.1 Traditional Protection	15
	3.3.2 Rip-rap Protection	15

Sl.No.	Particulars	Page No.
	3.3.3 Concrete Block Protection	16
	3.3.4 Gabion Mattress Protection	17
	3.4 Bridge Pier and Abutments	17
	3.5 Rainfall Erosion Control	19
11	Chapter 4 EXPERIMENTS AND EXPERIMENTAL RESULTS	20
12	Chapter 5 ANALYSIS AND DISCUSSION	32
	5.1 Velocity Decay	33
	5.2 Scour Characteristics	37
	5.2.1 Dynamic Scour Depth	37
	5.2.2 Static Scour Depth	39
	5.2.3 Radius of Scour Hole	42
	5.2.4 Scour Hole Profiles	45
	5.3 Performance of Geotextiles	50
13	Chapter 6 CONCLUSIONS AND SUGGESTIONS	56
	6.1 Conclusions	56
	6.2 Recommendation for future work	57
14	References	59

LIST OF FIGURES

Fig. No.	Title	Page
2.1	Bank Protection Scheme with Geotextile	10
3.1	Bonded Rip-rap Protection with Geotextile	16
3.2	Scour Protection for Bridge Pier with Geotextile	18
3.3	Scour Protection for Bridge Abutment with Geotextile	18
4.1(a)	Experimental Set-up	25
4.1(b)	Definition Sketch	25
4.2	Particle size Distribution Curves	26
5.1	Maximum Velocity Decay in Axial Direction	35
5.2	Velocity Decay in the Scour Hole	36
5.3	Increase in Dynamic Scour Depth (S_D) with Time (t)	40
5.4	Dynamic Scour Depth as a Function of F_j	41
5.5	Static Scour Depth ($S_{S_{oo}}$) as a Function of F_j	42
5.6(a)	Variation of r_{ooo}/H with $F_j/(H/\sqrt{A_j})$	44
5.6(b)	Variation of r_{ooo}/H with $F_j/P_1(H/\sqrt{A_j})$	44
5.7	Similarity of Dynamic Scour Profiles	46
5.8	Asymptotic Eroded bed Profiles (Static, $D=2.0$ mm)	47
5.9(a)	Dynamic Scour Profiles ($D=0.17$ mm)	48
5.9(b)	Similarity of Dynamic Scour Profiles	48
5.10(a)	Asymptotic State Eroded Bed Profiles (Static, $D = 0.17$ mm)	49
5.10(b)	Similarity of Static Scour Profiles	49
5.11	Increase in Depression of Geotextile with time	53
5.12	Bed Profile (Static) After Failure of Geotextile	54
5.13	Dynamic Bed Profiles with and without Geotextile	55

LIST OF SYMBOLS

A_j	Cross-sectional area of jet
D	Median size of bed material
F_j	Densimetric Froude Number = $U_j / \sqrt{gD \frac{\rho}{\rho_s}}$
F_o	Densimetric Froude Number = $U_o / \sqrt{gD \frac{\rho}{\rho_s}}$
H	Depth of impingement
F_1	Coefficient
R	Correlation Coefficient
S_D	Dynamic Scour Depth
S_S	Static Scour Depth
U	Axial velocity at any distance Z
U_j	Jet exit velocity
U_o	Jet velocity at original bed level
Z	Axial distance from jet exit
d_j	Diameter of jet
f	Function
g	Acceleration due to gravity
r	Radial distance from the axis of jet
r_o	Radius of scour hole at original bed level
r_r	Radial distance of ridge
x	Radius of scour hole at $0.5 S_{D\infty}$
t	Time from start of experimental run
ρ	Mass density of fluid
ρ_s	Mass density of sediment
ν	Kinematic viscosity of water
∞	Suffix to denote asymptotic state
	Values after failure

LIST OF TABLES

Table No.	Title	Page No.
1	Physical and Geometrical Characteristics of Bed Material	26
2	Experimental Observations	27

CHAPTER 1

INTRODUCTION

Erosion is the detachment and removal of rock and soil particles from their environment by the action of water. It constitutes the beginning of motion of particles that were previously at rest and their removal from the region under consideration.

On the basis of aerial extent and to a somewhat lesser degree on erosional intensity, erosion may be divided into land or soil erosion and local scour. Land erosion, an engineering problem applies primarily to the accelerated erosion of agricultural land. Local scour on other hand is used to describe those erosion phenomena involving a single unified flow pattern as e.g. the local scour around bridge piers, at the base of outlet structures, or by normally or obliquely impinging jets.

Most of the studies dealing with erosion and scour have been empirical because of the complexity of the physical process involved. Understanding of the scour problem has been aided considerably by investigations of scour by jets. When a

jet impinges on a bed of cohesionless material, scour process occurs through the kinetic energy of jet impact and by the forces generated by flowing water. The jet penetrates into the bed by scouring bed material out of the scoured hole and throws some of the scoured material all around the hole forming a ridge, rest of the scoured material remains in circulation by the high vorticity generated by jet. The process of removal and redeposition of bed material continues for a long time, with gradual deepening of scour hole. A limiting depth of scour is reached when rate of deposition of a bed material become equal to the rate of scour. When jet strikes bed of cohesionless material in unsubmerged condition, it gains more kinetic energy before striking the bed, but when submerged jet strikes the non-cohesive bed, it loses some of its energy before striking the bed in entraining the surrounding fluid.

The impingement of a jet on a surface finds application in a number of engineering problems. Jet issuing from hydraulic outlet works, weirs, vertical take off aircraft, the cavitating water jet drills, effluent discharge by jets are examples of such problems. On other hand, the prevention of damaging scour at the base of bridge piers and spill-ways is an important part of the design of hydraulic structures.

In the present work, submerged round jet has been used for scouring the beds of different sediment grades and geotextiles have been tested as scour protection device. The following chapter

reviews the work carried out by various researchers on scour by jets. Some information in brief about geotextiles are given in Chapter 3. Chapter 4 describes the experimental procedure and observations. The hydraulic characteristics of jet, its scouring action and performance of geotextile as scour protection measure are analysed in Chapter 5. Conclusions and the recommendations for further study are given in the concluding Chapter.

:::::

CHAPTER 2

LITERATURE REVIEW

Considerable research has been reported in studying the characteristics of submerged jets. Starting with the pioneering work of Rouse (1940), a number of studies have been made on the erosion of loose cohesionless material by submerged circular and plane jets, in the impinging and wall jet modes. Detailed review on the scouring by submerged jets are given by Rajaratnam.

2.1 Diffusion of Submerged Jets

Based on the studies by Albertson, Dai, Jensen and Rouse (1950) and Rajaratnam (1977), it was found that as the direct result of turbulence generated at the borders of a submerged jet, the fluid within the jet will undergo both lateral diffusion and deceleration, at the same time fluid from the surrounding region will be brought into motion. The diffusion process is dynamically similar and the longitudinal component of velocity within the diffusion region varies

according to the normal probability function at each cross-section. It is found that the potential core is followed by an axisymmetric type decay region in which velocity varies inversely with the axial distance and momentum is preserved, as the jet moves in forward direction.

2.2 Scouring Characteristics

Rouse (1940) conducted the first systematic study on scouring of nearly uniform fine sand by vertical submerged jet. Through dimensional analysis and Laboratory experiments, he found that the scour depth varied directly as the logarithm of duration of scour 't' for an appreciable part of the process and hence

$$\frac{S}{S_0} = m \log \frac{t}{t_0} \quad \dots \quad \dots \quad (1)$$

where,

S = the scour depth at t

S₀ = the scour depth at t₀ and,

m = the constant of proportionality depending on flow and sediment characteristics.

On the basis of equation (1) Rouse conducted that scour depth progresses without a limit for uniform sand. However, for graded sand the scour hole gradually got paved with coarser material and the scour depths obtained were less than those given by the logarithmic Law. The deviation

increased with time. The particles having fall velocities greater than jet velocity were termed as non-scourable particles.

Doddiah, Albertson and Thomas (1953) studied scour from jets and obtained an equation similar to the equation 21, and they concluded that a scour depth of any chosen magnitude can be reached provided the bed is allowed to be scoured for sufficient time. Their experiments were conducted upto $t = 120$ minutes.

Laursen (1952), showed that the limiting scour depth occurs when there is supply of sediment into the scour hole. He obtained an equation for scour depth variation with time and this equation when plotted with time on log scale approximates to a straight line over a considerable range hence to a logarithmic Law. Though his argument about the existence of limiting scour can not be disputed, his experiments, conducted upto a maximum duration of 300 minutes, do not show any deviation from logarithmic Law. The tendency of scour depth to reach a limit is not indicated by the experimental values.

Clark (1961) and Sarma Sivsankar (1967) report that the progress of scour is not strictly logarithmic and constants involved for logarithmic laws are not easily predictable. Ahmad's (1953) experiments on scour below the apron of a weir also show

that after some long initial time, the scour depths deviate from the logarithmic law such that they are less than those given by extrapolating the logarithmic law.

Carsten (1966), in his study on similarity laws for localised scour, gave the relation

$$\frac{\text{(sediment out flow from scour)}}{\text{hole per second}} - \frac{\text{(sediment inflow into the)}}{\text{scour hole per second}} = \frac{d}{dt} \text{(Vol. of scour hole)...(2)}$$

On the basis of this equation, he concluded that scour progresses without limit as time tends to infinity, when there is no sediment supply to the scour hole and on the other hand reaches a limit when there is sediment supply. This means that for all values of sediment supply including those tending to zero, the limiting scour depth is finite and for the value of sediment supply equal to zero, it shoots upto infinity. Any such double valued functions for scour process are inadmissible.

Sarma, Sivsankar (1967) and Sarma (1967) concluded that the true scour-time relationship should be such that

- (i) It gives zero scour depth when $t = 0$
- (ii) at any time, $\frac{ds}{dt}$ is a positive quantity, however, small it is.
- (iii) A limit exists for scour depth, but is reached only asymptotically when all the variables except time are kept constant, and

(iv) It approximates to a logarithmic relationship.

They concluded that the scour depth is a tangent inverse function of time and that the limit exists for scour depth. The progress of scour approximates to a logarithmic law in two adjoining ranges of time.

Erosion caused by submerged circular air jets impinging on loose bed of sand and polystyrene was studied by Rajaratnam and Beltaos (1977) and based on their study, they found that S_s , the static depth of erosion and radius at which the depth of scour was zero, in terms of H , the impingement height, were mainly function of $F_j/(H/d)$ for large H , in which the densimetric Froude number $F_j = U_j / \sqrt{gD \frac{\Delta\rho}{\rho}}$, where U_j = jet velocity, g = acceleration due to gravity, D = the median grain size, ρ = the density of fluid and $\Delta\rho$ = the difference between the densities of sediment and the fluid.

Erosion by submerged circular jets was also studied by Rajaratnam (1982). Rajaratnam and Berry (1977) studied the erosion produced by submerged circular wall jets of air and water on the beds of polystyrene and sand. They found that the characteristic lengths of erosion process in terms of the jet diameter ' d ' were function of only F_j . Further the eroded bed profiles were found to possess the property of geometrical similarity.

Rajaratnam and Roger, K. Macdougall (1983) and Rajaratnam (1981) studied erosion by planewall jets with minimum tail water.

Walter and Kabir (1983) studied the effects of impingement of submerged water on non-uniform stream bed through laboratory experiments and theoretical analysis. They found that the scour depth was influenced by gravel gradation and armor action, the scour depth was reduced due to armor action.

Recently, Dwivedi (1988) studied the scour phenomena on sand beds of uniform grain size by submerged annular water jets. He found the presence of vortex type of flow in the scour hole. He found that the scour hole deepens with time but finally reaches a stable state, this limiting scour depth is a function of F_o , depth of submergence and grain size of sediment.

2.3 Scour Control

Erosion of natural embankments of a river, canal or shore lines of sea is a common phenomenon due to the action of flowing water. In certain cases, depending upon the nature of soil the erosion can be severe and so fast that it begins to endanger nearby inland structures of their very foundations. Local erosion due to intensive action of flow can be termed as scour. The traditional method of controlling scour is to shield the particles from the moving water with a flexible

protective structure. Rip-rap (broken rocks) or heavy armour stones, concrete blocks articulated concrete mattresses are some of the traditional structures that can be utilised for scour protection. To prevent the loss of underlying soil, a graded aggregate filter is used between the natural soil and protective covering. Posey (1974) studied performance of protection work for prevention of scour around the bridge pier on scale model with inverted filter and found better performance than that for protection without filter. But the difference in particle size between the natural soil and protective covering could make the use of as many as five layers of differently graded aggregates necessary in such granular filter. It can prove difficult and expensive to install a multi-layer erosion protection and filtration system. The use of a geotextile filter can simplify construction of the erosion control measures as illustrated in figure.



Fig. 2.1 Bank Protection Scheme with Geotextile

Godbole and Mehendale (1989) conducted experiment with Nylon filter in place of inverted graded filter and found no scour around the pier and also no displacement of blocks provided on the Nylon filter.

Details of protection work using geotextiles and their performance are given by Jain (11) and Roemer (19).

No work has been reported on geotextile as protection measure to control scour due to water jets. A brief review of geotextiles and their use in scour and erosion protection is given in Chapter 3.

:::::

CHAPTER 3

THE ROLE OF GEOTEXTILES AS AN EROSION CONTROL DEVICE

3.1 Geotextiles in Perspective

Geotextiles are defined as permeable textiles used in conjunction with soil or rocks, as an integral part of man made project. Geotextiles are used in a wide range of applications, the main applications are erosion control, soil filtration, road sub-base separators, reinforcing soils in embankments and retaining walls.

3.1.1 Basic Geotextile Functions

Four basic functions of geotextile are identified namely separation, filtration, reinforcement and drainage. These basic functions can be summarised as follows. When used as separator, the geotextile must prevent the intermixing of particles from two soil layers with different properties. This

prevents contamination which can impair the intended behaviour of granular soil layer. Where it is to be used for liquid transmission, the geotextile itself must provide the drainage medium for water or gas to flow out of the soil. If it is to act as reinforcement, the geotextile must have sufficient strength and surface bond to hold the soil mass together. Where its role is that of filtration the geotextile must promote the development of a natural filter in the adjacent soil, holding back the other soil particles while at the same time allowing the water to pass through.

The selection of suitable geotextile for a particular design is based upon matching the geotextiles ability to perform each of the basic functions to their relative importance in that design applications.

3.2 Types of Geotextile

3.2.1 Raw Materials

The four main polymer families most widely used as the raw material for geotextile are :

- (i) Polyester
- (ii) Polyamide
- (iii) Polypropylene
- (iv) Polyethylene.

Although most geotextiles are made from synthetic polymers, a few specialist geotextiles may incorporate either steel wire or natural biodegradable fibres.

3.2.2 Woven Geotextile

Geotextiles can be subdivided into several different categories based on their method of manufacture. Woven textiles were the first to be developed from synthetic fibres. As their name implies, these geotextiles are manufactured using weaving techniques adapted from those used to weave clothing textiles. It is generally found that woven geotextiles have a relatively high strength and a relatively low extensibility when compared to other types of geotextiles of the same weight.

3.2.3 Non-woven Geotextile

There are three main subdivisions of this type of geotextile, based upon the way in which the geotextile fibres are bonded together - namely thermally bonded, chemically bonded and mechanically bonded. The random distribution of the filaments of non-woven geotextiles contains a wider range of opening sizes than is found in a woven geotextile. The absence of any preferred orientation to the filaments also gives the non-woven geotextile a more isotropic strength. These geotextiles are usually 2 to 5 mm thick.

Some other commonly used types of geotextiles are knitted geotextiles, polymer nets and mats, strips webs, ties, biodegradable geotextile and composites, etc.

3.3 Erosion Control

3.3.1 Traditional Protection

Rip-rap or heavy armour stones, concrete blocks etc. are some of the common traditional protections device used as around hydraulic structures. The weight of these devises helps the soil particles in the banks or beds to resist the effect of any seepage into waterway. However, the protective material is usually required to be permeable in order to prevent the build up of hydrostatic pressure. The drainage openings which can be very large in case of rip-rap would expose the underlying soil to erosion. To prevent erosion geotextiles can be used in place of traditional inverted graded filters.

3.3.2 Rip-rap Protection

In West Germany, the Federal Institute for Waterways Engineering has established standard designs for protecting the banks of waterways. Fig. 3.1 shows the most widely used system of protection which is bonded rip-rap laid over a layer of thick composite geotextile. This is intended for use on the banks of waterways which have a side slope between 1 in 4 and 1 in 3 and a maximum vessel size of 1350 tonnes.

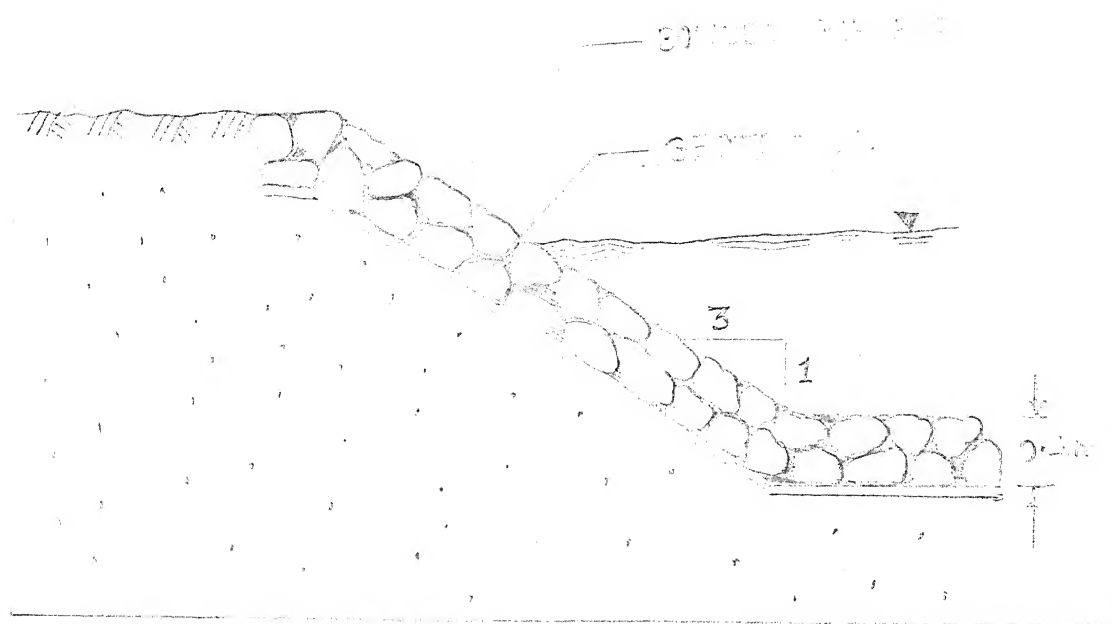


Fig. 3.1 Bonded Rip-rap protection with Geotextile

In some soils, there is a tendency for the particles to become loosened in the wave zone even when protected by geotextile and the rip-rap. Without precautions, the loosened soil particles may move down the slope to produce a bulge and a depression in the protection work. This problem can be avoided by using a composite geotextile.

3.3.3 Concrete Block Protection

Heavy closely fitting concrete unbonded blocks are used for erosion control. If some means of linking the concrete block together is utilised, then this additional integrity enables a lighter weight of concrete block to perform in a similar manner to a heavier weight of rip-rap protection.

By using two orthogonal sets cables to link the individual blocks together, a flexible articulated panel is created which can be laid over the geotextile filter.

3.3.4 Gabion Mattress Protection

Gabion are the mesh baskets, which are filled with relatively small rocks. The gabion mesh prevents these small rocks from being washed away by wave action as it completely encases them. This form of construction also ensures that gabion are inherently permeable and flexible.

3.4 Scour Protection

Flow of water over an obstruction causes a local increase in water velocity, together with eddies and vortices. This can cause the erosion of the stream bed sediment to be concentrated around structures such as pipelines, oil and gas production platforms, bridge abutments and piers.

3.4.1 Bridge Pier and Abutments

Scour protection around bridge piers and abutments often consists of a covering of large rip-rap stones around their base, separating the scour susceptible sediments from the water currents. A geotextile sheet laid beneath the rip-rap provides additional protection by limiting any tendency for the sediments to wash into the rip-rap.

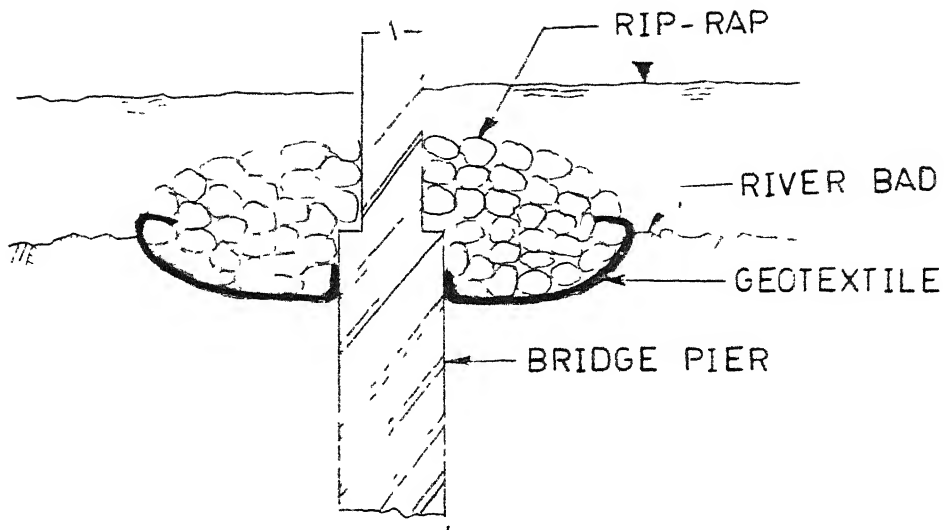


FIG. 3-2 SCOUR PROTECTION FOR BRIDGE PIER
WITH GEOTEXTILE

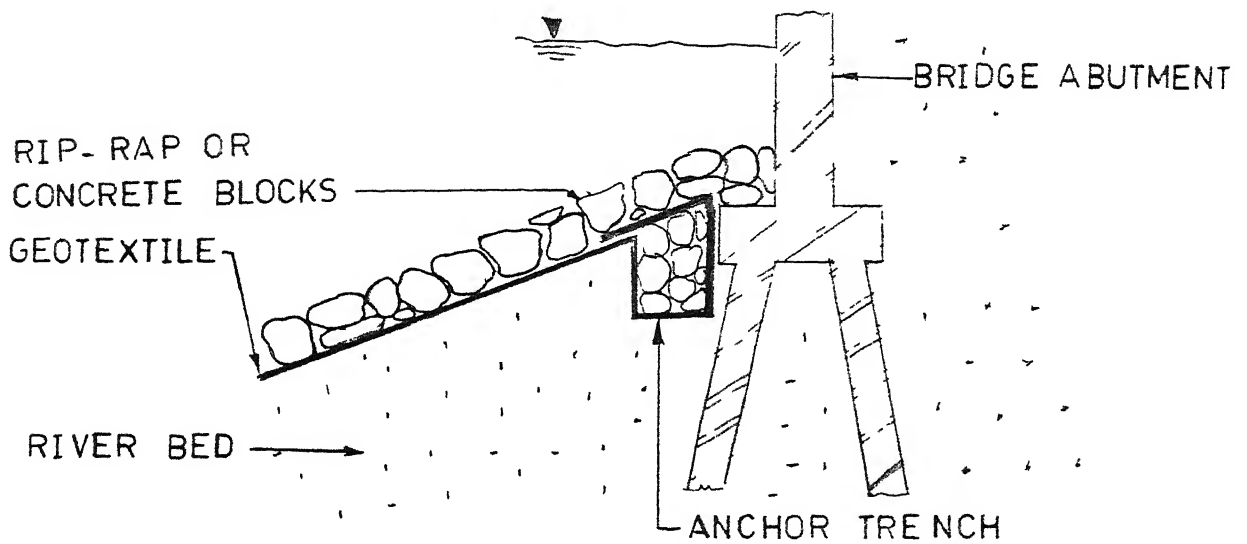


FIG. 3-3 SCOUR PROTECTION FOR BRIDGE ABUTMENT
WITH GEOTEXTILE

Fascine mattress, prefabricated ballast mattress are used in seabed protection work. Polypropylene trends have been used as artificial seaweed in sea bed scour protection work since about 1963.

3.5 Rainfall Erosion Control

On steep ground with little or no covering of vegetation, rainfall erosion can be a major problem. Common geotextiles for rainfall erosion control or special biodegradable geotextiles for providing temporary cover to soil can be used.

: : : : :

CHAPTER 4

EXPERIMENTS AND EXPERIMENTAL RESULTS

The experimental investigation has been carried out with a test set up as shown in Fig. 4.1.

A cylindrical tank of diameter 57 cm and height 90 cm was filled with sand of the required size. This tank was put concentrically within larger tank of diameter 75 cm and height 110 cm. Thus there was an annular space of 9 cm between the inner and outer tanks worked as a sediment trap. The impinging jet was provided by a 2.5 cm diameter nozzle fitted at lower end of a 7.5 cm diameter vertical pipe. This vertical pipe of diameter 7.5 cm was connected to the horizontal pipe of the same diameter which draws water from an overhead reservoir, thus providing supply at constant head during arun. Flow straightners were inserted in the vertical portion of the 7.5 cm diameter pipe to produce a symmetrical jet. In the horizontal portion of the pipe a sluice valve was provided to regulate the discharge from the jet.

An outlet for water was provided on the outer tank, which discharged the water to a v-notch tank used to measure the discharge. The position of nozzle of the jet was fixed, the submergence levels were varied by changing the height of the sediment bed above the bottom of the inner tank.

The experiments were conducted with the 2.5 cm diameter nozzle. Two types of sands with mean size D (50 % finer than this size) of 2.0 and 0.17 mm were used. The physical and geometrical characteristics of bed materials are summarised in Table-1.

The erosion process for both the sands with and without geotextile was observed from beginning to the asymptotic state. In all these experiments, the depth of water was always above the jet exit, which itself submerged the grains.

The velocity heads of the jet at different axial distance from the jet exit were measured with the help of pitot tube of diameter 1.2 mm. The velocity heads were measured in terms of height of water column.

The maximum scour depth at centre of the scour hole, dynamic as well as static scour profiles in asymptotic state were taken with the help of point-gauge with flat bottom.

The assemblies for measuring velocity heads and scour hole profiles were mounted on a travelling bridge capable of being rotated in any direction.

For each run the maximum depth of scour was measured at different time intervals. The dynamic profiles in asymptotic state were measured in eight different radial directions at intervals of 45° around the jet axis.

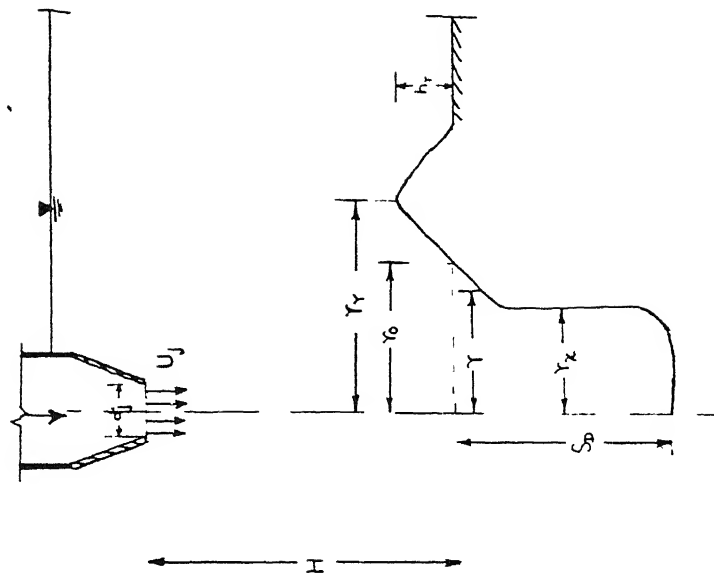
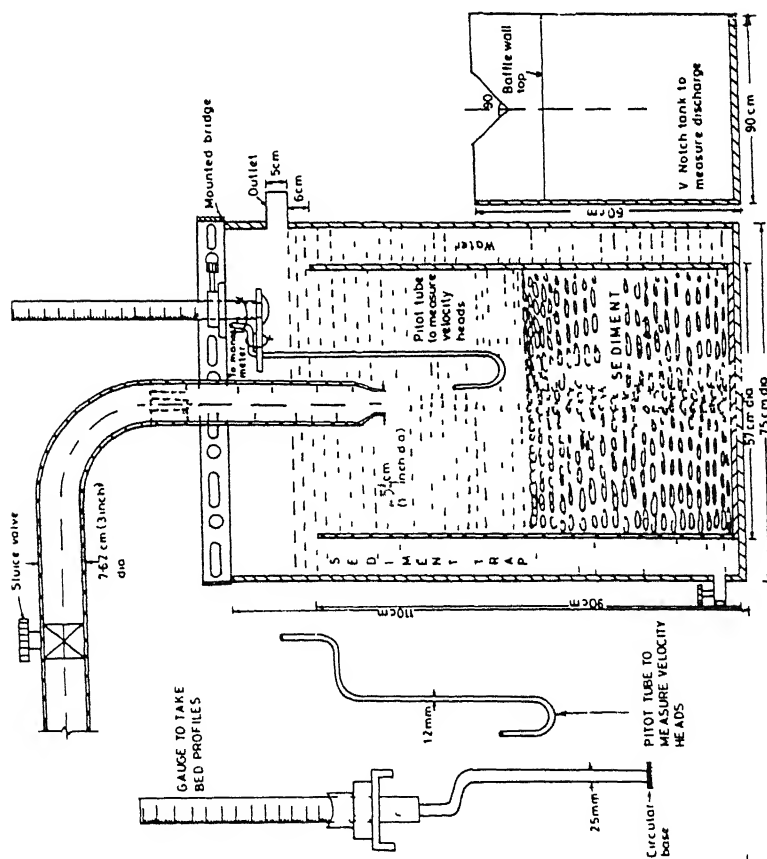
After stopping the discharge from the jet the static profile for each run were measured in four radial directions. During this study, it was recognised that the scour or erosion observed after the jet is stopped could be significantly different from the erosion profile that exists with the jet on. The erosion depth with the jet on is referred to as the depth of dynamic scour, S_D , whereas the depth of erosion observed after the jet is stopped is referred to as static depth of erosion ' S_s '. While the static erosion profile was easily measured with the point gauge, the measurement of dynamic profile needed a lighting arrangement.

Two series of experiments were conducted for 2.0 mm sand. In the first series submergence level H measured from bed level to jet exit was maintained constant and jet velocity U_j was varied. In the second series flow velocity of the jet was kept constant and the submergence level was varied. Third series of experiments

were conducted with 0.17 mm sand (Ganga sand) in which the submergence level was kept constant and jet velocity was varied. In the fourth series of experiments, the Geotextile was tested as a scour protection device. The geotextiles were cut into circular shape.

In each run, the geotextile was anchored on the sand bed with U-pin anchors concentrically with jet axis. The length of U-pin limbs was 10 cm, with 2 cm gap between them. Anchors were pressed through the geotextile into the sand bed perpendicularly. The U-pin anchors were placed in radii 7.5 cm and 12.5 cm with the c/c spacing of 5.0 cm on inner radius and in staggered way on outer radius. Before starting the jet, the level of geotextile was noted. When the jet was on, the level of depression at centre line of jet was recorded at different time intervals. Each time the anchors were checked for proper anchorage. The failure of geotextile is considered when warping of geotextile takes place due to piping below geotextile and lifting of anchors occur. In another series of experiments, geotextile was kept 5 cm and 10 cm below the bed level and experiments were repeated with constant submergence level ' H ' and jet velocity ' U_j '. In steady state, the surface profiles of geotextile with jet on and jet off conditions were measured.

Summary data of experiments are given in Table 2.
All relevant data are presented in graphical form in
Chapter 5.



HALF SECTIONAL VIEW
FIG 41(b) DEFINITION SKETCH

Table 1. Physical and Geometrical Characteristics of the Bed Materials.

Bed material	Median grain size D (mm)	Specific Gravity P_s	Angle of Repose ϕ (in degree)
Yamuna sand	2.00	2.50	29°44'
Ganga sand	0.17	2.78	30°00'

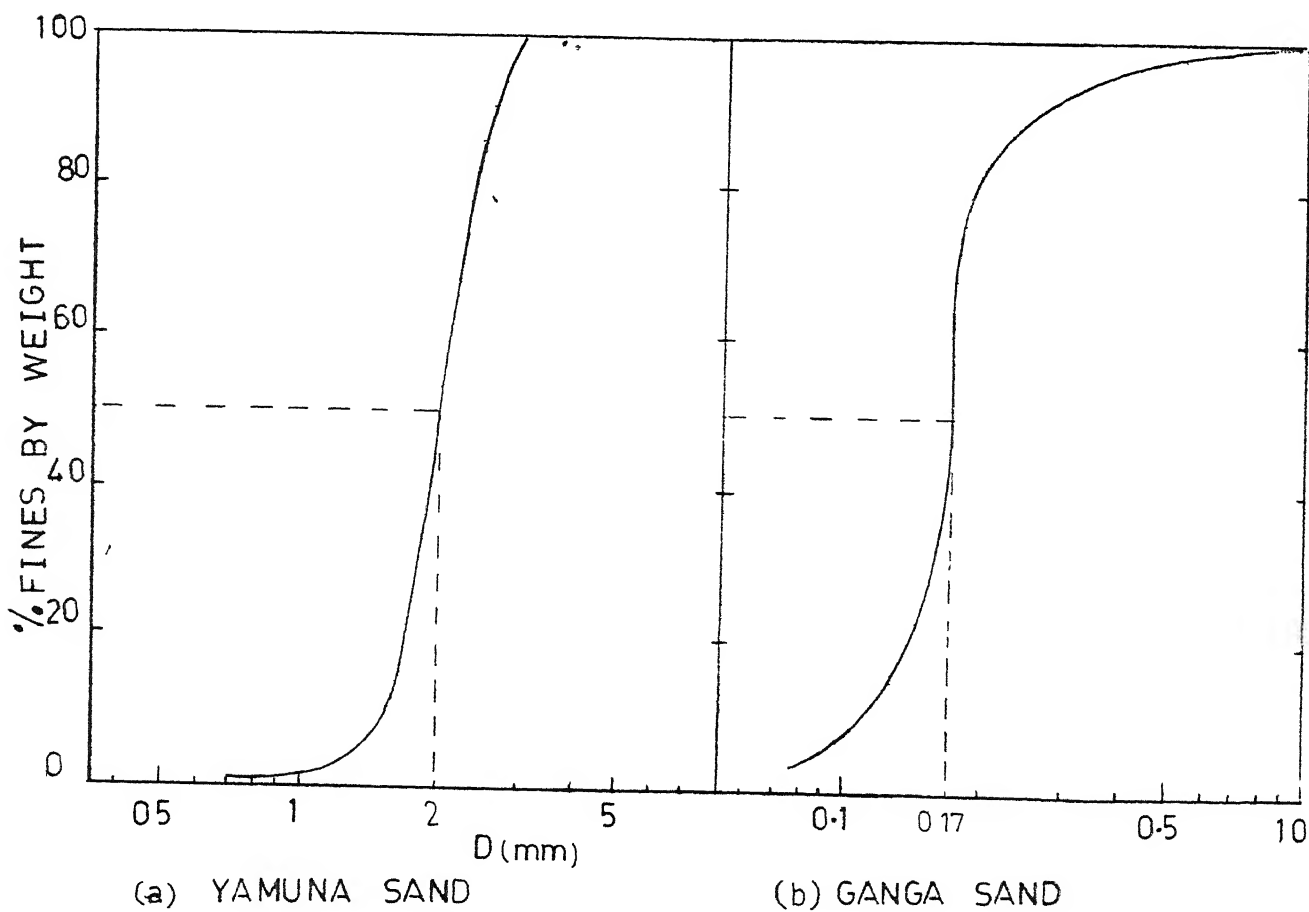


Fig. 4.2 Particle size distribution curves.

Table 2. Experimental Observations

Table 2(a): For Yamuna Sand, $D = 300 \text{ mm}$

$$P_s = 2.50$$

$$\phi = 30^\circ.00$$

$$d_j = 2.54 \text{ cm}$$

$$\gamma = 0.9134 \times 10^{-6} \text{ m}^2/\text{sec at } 25^\circ\text{C (average)}$$

$$P_1 = 0.80$$

Expt.	H cm	U_j m/sec	F_j	F_o	$S_{D_{\infty}}$ cm	$S_{D_{\infty}}/H$	$S_{S_{\infty}}$ cm	$S_{S_{\infty}}/$
1	12.50	1.10	6.41	5.42	5.25	0.42	3.41	0.27
2	12.66	1.58	9.20	8.52	8.54	0.67	3.79	0.30
3	12.50	1.81	10.55	9.50	10.50	0.84	3.90	0.31
4	12.50	2.43	14.16	13.24	16.50	1.32	5.20	0.42
5	12.40	3.17	18.48	16.79	21.30	1.72	5.80	0.47
11	14.20	2.36	13.76	12.88	15.00	1.06	4.70	0.33
12	16.25	2.37	13.82	12.41	13.80	0.84	4.60	0.28
13	18.50	2.35	13.70	10.72	13.50	0.73	4.40	0.24
14	21.10	2.34	13.64	10.49	12.90	0.61	4.20	0.20
21	18.00	2.81	16.38	12.24	14.80	0.82	5.80	0.32
22	18.00	3.68	21.45	15.16	19.90	1.11	6.00	0.33
23	18.00	4.96	28.91	23.14	29.60	1.64	6.30	0.35

xpt.	r_{∞}	r_{∞}	r_r	h_r	$\frac{U_{\infty} d_1}{\sqrt{v}}$	$\frac{F_1}{(H/\sqrt{A_j})}$	$\frac{F_1}{P_1 (H/\sqrt{A_j})}$	$\frac{r_{\infty}}{H}$
	cm	cm	cm	cm	$\times 10^4$			
1	8.00	4.70	6.00	1.5	3.06	1.15	1.44	0.37
2	9.45	5.00	10.00	2.2	4.39	1.63	2.04	0.39
3	9.50	5.25	10.50	2.0	2.03	1.90	2.37	0.42
4	10.6	5.50	11.00	1.8	6.76	2.55	3.18	0.44
5	17.00	7.00	14.00	2.3	8.83	3.35	4.18	0.56
11	11.00	5.20	10.40	1.7	6.56	2.18	2.72	0.37
12	11.30	5.00	10.00	2.4	6.59	1.91	2.39	0.31
13	11.50	5.00	10.00	1.9	6.54	1.67	2.09	0.27
14	12.00	6.00	12.00	2.5	6.51	1.46	1.82	0.28
21	11.85	6.50	11.70	2.5	7.81	2.05	2.56	0.36
22	15.60	6.30	13.00	2.9	10.23	2.68	3.35	0.35
23	-	7.40	14.80	3.5	13.80	3.62	4.52	0.41

Table 2(b) Ganga Sand

$D = 0.17 \text{ mm}$

$P_s = 2.78$

$\phi = 29^\circ.44$

$d_j = 254 \text{ mm}$

$\nu = 0.77 \times 10^{-6} \text{ m}^2/\text{sec. at temp.} = 33^\circ\text{C}$
(average)

$P_1 = 0.44$

Expt.	H cm	U_j m/sec	F_j	F_o	$S_{D\infty}$ cm	S_D/H	$S_{S\infty}$ cm	$S_{S\infty}/H$
31	12.50	1.05	19.24	14.54	15.63	1.25	-	-
32	12.50	1.56	28.63	26.80	31.25	2.50	7.40	0.59
33	12.50	1.80	38.40	31.94	35.00	2.80	-	-
34	12.50	1.78	32.67	31.75	34.50	2.76	7.80	0.62
35	12.50	4.62	84.79	80.02	40.00*	3.20	-	-
36	10.00	1.78	32.67	32.12	37.50	3.75	9.6	0.96

Expt.	r_{∞}	$r_{0\infty}$	r_x	H_r	$\frac{U_{\infty} d_1}{\nu}$ $\times 10^4$	$\frac{F_1}{H/\sqrt{A_j}}$	$\frac{F_1}{P_1(H/\sqrt{A_j})}$	$\frac{r_{0\infty}}{H}$
31	19.00	14.00	7.60	3.3	3.46	3.46	7.89	1.12
32	22.00	15.50	8.70	4.1	5.15	5.16	11.76	1.24
33	25.00	16.00	9.50	-	5.94	5.95	13.56	1.28
34	28.00	18.30	9.00	5.5	5.87	5.88	13.40	1.46
35	-	-	-	-	15.24	15.27	34.80	-
36	28.00	17.75	10.00	5.4	5.87	7.35	16.75	1.80

Table 2(c) Experiments with Geotextile

Expt.	Type of Geotextile	Elevation of Geotextile w.r.to sand bed cm	D mm	H cm	U _j m/sec	F _j	F _o	S _D cm	S _S cm
41	GPB 127	0.00	2.00	18.00	2.31	13.47	10.78	0.65	0.60
42	GPB 127	0.00	2.00	18.00	2.80	16.32	-	0.30	0.30
43	GPB 127	0.00	2.00	18.00	4.97	28.97	-	8.30*	8.20
51	GPB 127	0.00	0.17	12.50	1.78	32.67	31.50	1.80	1.30
52	GPB 127	0.00	0.17	12.50	4.62	32.67	31.53	13.70*	7.50
53	GPB 127 (with reinforcement down)	0.00	0.17	10.00	1.78	32.67	32.12	13.70*	9.60
54	GT6	0.00	0.17	12.50	4.62	84.79	82.18	6.00*	6.00
55	GT6	-5.00	0.17	12.50	4.62	84.79	82.05	6.90	5.10
56	GT6	-10.00	0.17	12.50	4.62	84.79	82.20	11.40	1.30
57	425B	0.00	0.17	12.50	4.62	84.79	82.20	8.30	8.10
58	425B	-5.60	0.17	12.50	4.61	84.61	81.88	8.00	6.60
59	425B	-10.00	0.17	12.50	4.61	84.61	81.88	12.00	1.20
60	425C	0.00	0.17	12.50	4.61	84.61	82.03	5.40	4.90
61	425C	-5.00	0.17	12.50	4.61	84.61	80.00	5.40	4.00
62	425C	-10.00	0.17	12.50	4.61	84.61	82.04	10.60	0.70
63	425C	0.00	0.17	12.50	4.61	84.61	81.90	6.8	-
64	425C	-5.00	0.17	12.50	4.61	84.61	82.04	5.8	4.2
65	425C	-10.00	0.17	12.50	4.61	84.61	82.04	12.7	0.4

CHAPTER 5

ANALYSIS OF RESULTS

In view of the complexities of the problem due to mobile bed hindering the jet flow, a complete theoretical solution of the problem of local scour by jets is not possible. An experimental investigation of the problem has been carried out to obtain empirical relationships for flow characteristics and scour properties. The variable experimental parameters considered in the analysis are the jet velocity at exit U_j , submergence depth H , median grain size of the sediment D , mass density of the sediment ρ_s , and the kinematic viscosity of water ν .

The functional relationships for the decay of center line velocity of jet with distance, scour characteristics of the bed in dynamic and static conditions, have been derived from the experimental data in terms as described in the following sections.

5.1 Velocity Decay

As the jet flows out from the nozzle, it entrains the surrounding fluid, causing reduction in the centre line velocity after the potential core region. This reduction in velocity increases with increase in axial distance. From the principle of conservation of moment, it has been shown that the total momentum of the jet remains constant along the axial distance. The maximum velocity decays linearly with increase in axial distance. This state of jet flow is valid till the jet strikes the sediment bed. Once the jet strikes the sediment bed, due to intense erosion, the sediment is scoured out forming a hole around the jet.

The deepening and widening of the scour hole continues till an equilibrium state is reached. The equilibrium state may be defined as the state at which no net erosion takes place or erosion equals the deposition of sediment occurring due to vortex flow between the jet boundary and scour hole boundary. This vortex compresses the jet and may confine the jet all around. Due to this confinement of jet the growth of jet boundary and decay of centre line velocity below original bed level in the scour hole may be different from that above the scour hole. In order to study decay of centre line velocity, measurement of velocity at different axial distance from jet exit was carried out using pitot tube. The values of centre line velocity U , normalised with

velocity at jet exit U_j are plotted against the corresponding values of axial distance Z , normalised with square root of the cross-sectional area, A_j , of jet exit as $Z/\sqrt{A_j}$, as shown in Fig. 5.1. From Fig. 5.1, it is clear that the U_j/U remains unity till $Z/\sqrt{A_j} \approx 5$ and then increases with $Z/\sqrt{A_j}$. The zone $Z/\sqrt{A_j} < 5$ can be termed as potential core region or developing region. The zone $Z/\sqrt{A_j} > 5$ is developed zone. Fig. 5.1 shows that in the zone of established flow, the velocity decays linearly with the axial distance Z . The regression equation, using method of least square fit, for velocity decay in established flow region is

$$\frac{U_j}{U} = 0.610 + 0.077 \frac{Z}{\sqrt{A_j}} \quad \dots \quad \dots \quad \dots \quad (5.1)$$

with correlation coefficient $R = 0.97$.

In order to study the decay of the centre line velocity of jet, in the confined zone of scour hole, the plot of $\frac{U_o}{U}$ is made against $\frac{Z-H}{H}$ in Fig. 5.2, where U_o = centre line velocity at the original bed level and H = depth of impingement measured as the difference in levels of jet exit and original bed level. The jet impingement depth 'H' is used instead of $\sqrt{A_j}$ as used in Fig. 5.1, because the jet width at the bed striking level is proportional to H . From the plot, it is observed that this velocity also varies linearly with axial distance. Trend of velocity decay in the scour hole is represented by a straight line.

$$\frac{U_o}{U} = 0.9663 + 0.6764 \left(\frac{Z-H}{H} \right) \quad \dots \quad \dots \quad \dots \quad (5.2)$$

with $R = 0.94$

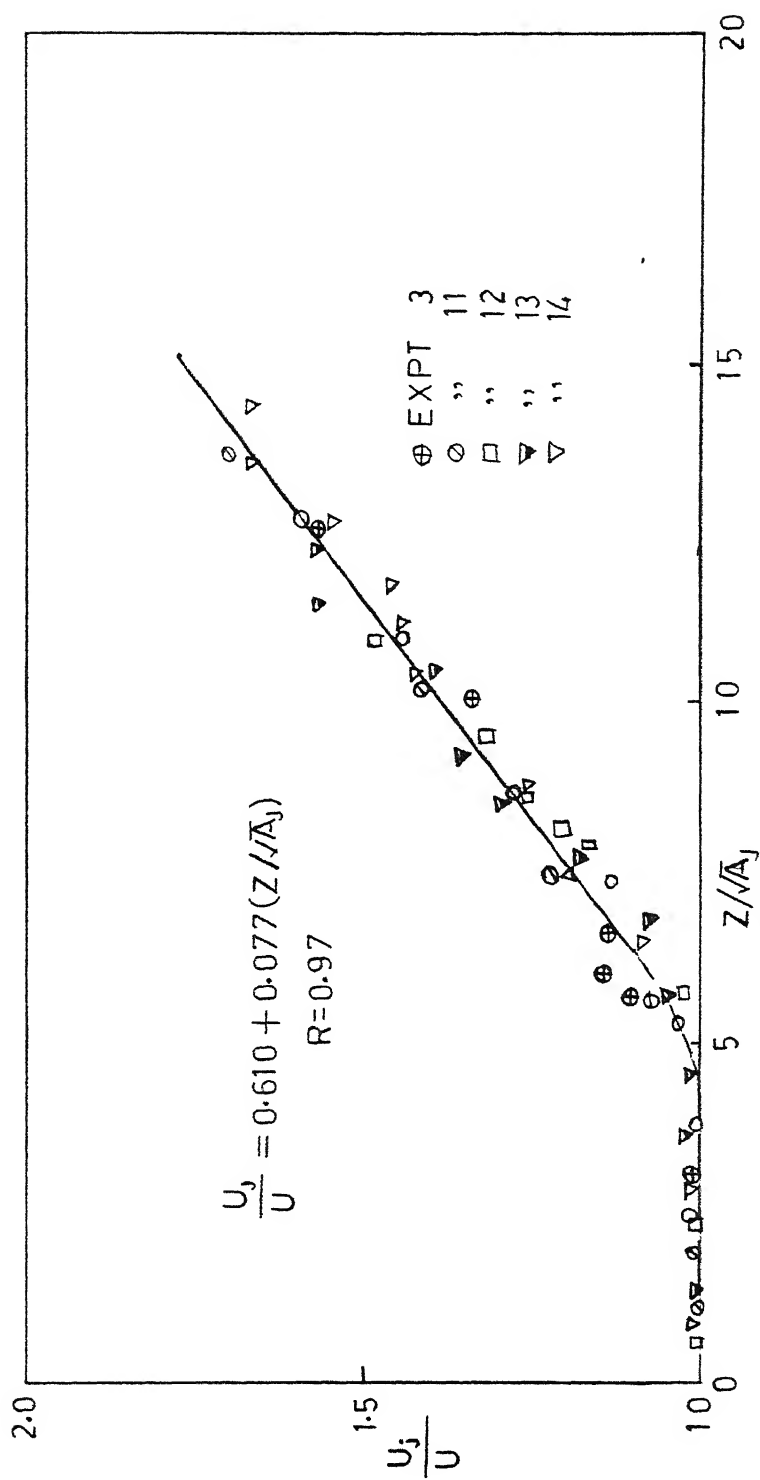


FIG. 51 MAXIMUM VELOCITY DECAY IN AXIAL DIRECTION

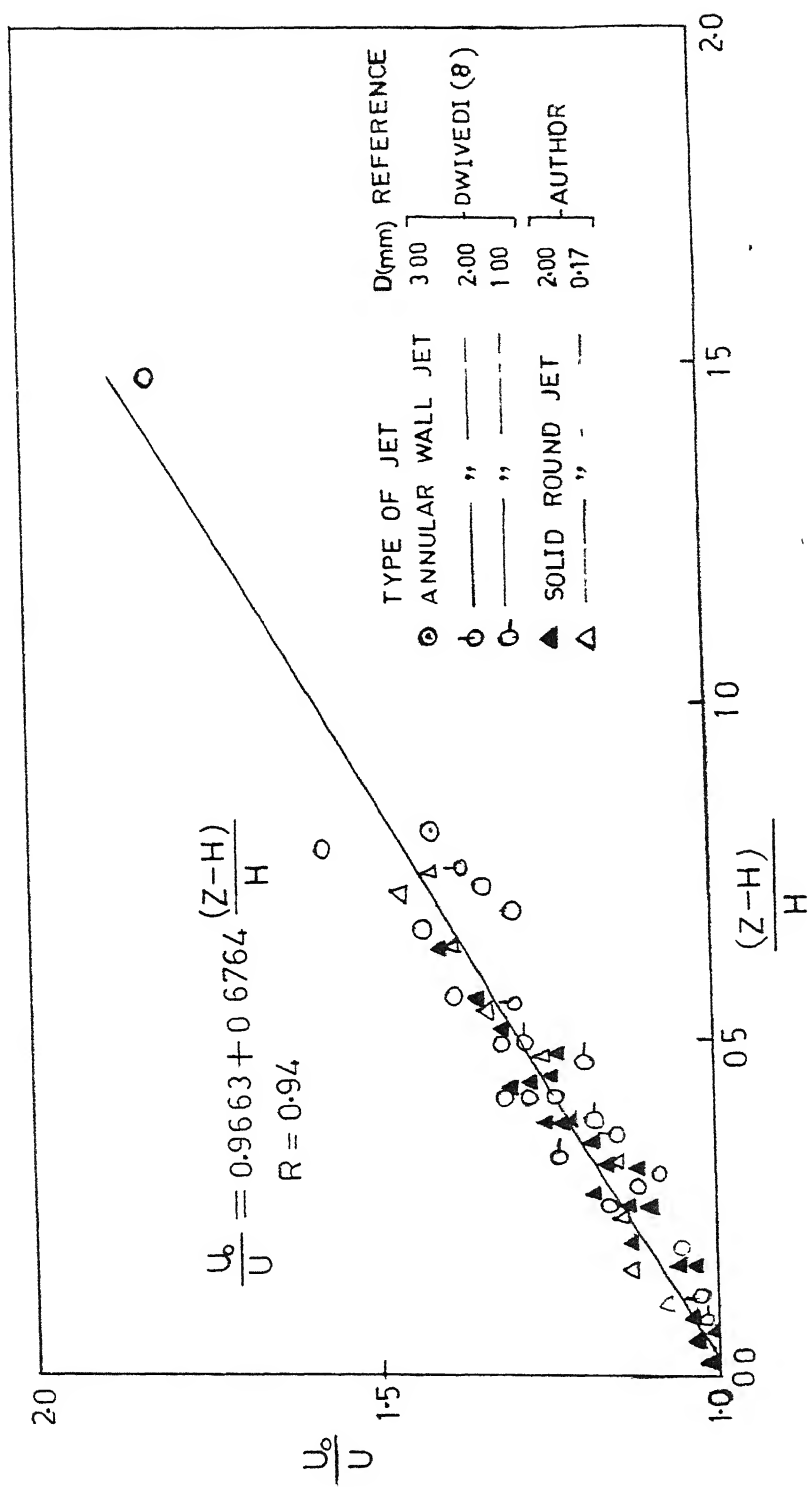


FIG 5-2 VELOCITY DECAY IN THE SCOUR HOLE

5.2 Scour Characteristics

The jet issuing from the nozzle, quickly penetrates the sand bed nearly the full depth of the scour hole then it deflects back from the bottom of the hole. Returning water carries scoured material with it and throws over the bed. Some of the material, thrown out, forms a ridge, all around the scour hole, while the remaining portion remains in suspension. The material thrown down-stream of the ridge stays there but the material upstream of the ridge slides along the slope into the scour hole and gets entrained into the water in the scour hole and again gets thrown out of the hole. Initially depth of scour hole increases with time, after some time depth becomes constant. When the jet is stopped, the material upstream of the ridge slides quickly, into the scour hole, whose sides attain an inclination angle equal to its natural angle of repose.

5.2.1 Dynamic Scour Depth

The growth of the dynamic scour depth at the centre, S_D , with time, is shown in Fig. 5.3, which shows that initially S_D increases linearly with $\log t$. After certain time, the variation of S_D with t deviates from this logarithmic trend to finally approach the asymptotic value of $S_{D_{\infty}}$. Fig. 5.3 shows that for

fine sediment bed ($D = 0.17$ mm), scour depth reaches to asymptotic state earlier than the coarser bed ($D = 2.00$ mm).

Considering the maximum depth of scour hole, $S_{D_{\infty}}$, one can write a functional relationship.

$$S_{D_{\infty}} = f_1 [U_j, \rho, H, A_j, D, g\Delta\rho, \nu] \quad (5.3)$$

in which U_j = jet velocity at nozzle, ρ = the mass density of fluid, H = height of impingement, A_j = cross sectional area of nozzle, $\Delta\rho$ = the different of mass density of the bed material and the fluid, g = acceleration due to gravity and ν = the kinematic viscosity of the fluid. Using dimensional analysis Equation 5.3 can be reduced to

$$\frac{S_{D_{\infty}}}{D} = f_2 \left[F_j, \frac{U_j d_j}{\nu}, \frac{H}{D}, \frac{H}{\sqrt{A_j}} \right] \dots \dots (5.4)$$

in which $F_j = U_j / \sqrt{g(\Delta\rho/\rho)D}$ = densimetric Froude number of the system. For larger values of Reynolds number (greater than a few thousand), the effect of visocisty can be neglected and Equation 5.4 can be reduced to

$$\frac{S_{D_{\infty}}}{D} = f_3 \left[F_j, \frac{H}{\sqrt{A_j}}, \frac{H}{D} \right] \dots \dots \dots (5.5)$$

Dynamic scour depth depends on the flow conditions at the original bed level. This can be taken into account by modifying the functional term of Equation 5.5 as

$$\frac{S_{D_{\infty}}/D}{H/D} = f_4 \left[\frac{F_j}{H/\sqrt{A_j}} \right] \dots \dots \dots (5.6)$$

$$\text{or } \frac{S_{D_{\infty}}}{H} = f_5 \left[\frac{F_j}{H/\sqrt{A_j}} \right] \quad \dots \dots \dots (5.7)$$

where $S_{D_{\infty}}$ represents the scour depth normalised with the jet width at the original bed level. The experimental observations on the depth of erosion for the asymptotic state are plotted in Fig. 5.4. The wall jet data of Dwivedi (8) for water-sand and circular jet data of Rajaratnam for air-sand, air-polystyrene (14) and water-sand (18) are also shown in figure. The regression line, drawn through the data points in figure 5.4, is described by the equation

$$\frac{S_{D_{\infty}}}{H} = -0.0616 + 0.4461 \frac{F_j}{(H/\sqrt{A_j})} \quad \dots \dots (5.8)$$

$R = 0.96$

Extrapolation of the straight line in figure 5.4, shows that for $(S_{D_{\infty}}/H) = 0$, $F_j/(H/\sqrt{A_j})$ has a positive value. This indicates the presence of resistance in cohesionless bed materials against erosion and that the initiation of scour occurs only when flow conditions had attained certain critical values. In this study, the critical value of $F_j/(H/\sqrt{A_j}) \approx 0.1381$.

5.2.2 Static Scour Depth

The static scour depth ($S_{S_{\infty}}$) is measured as the difference in the original bed level to the deepest portion of the scour hole after the jet is stopped. As in the case of dynamic scour depth, the static scour depth $S_{S_{\infty}}$ can also be shown by the equation

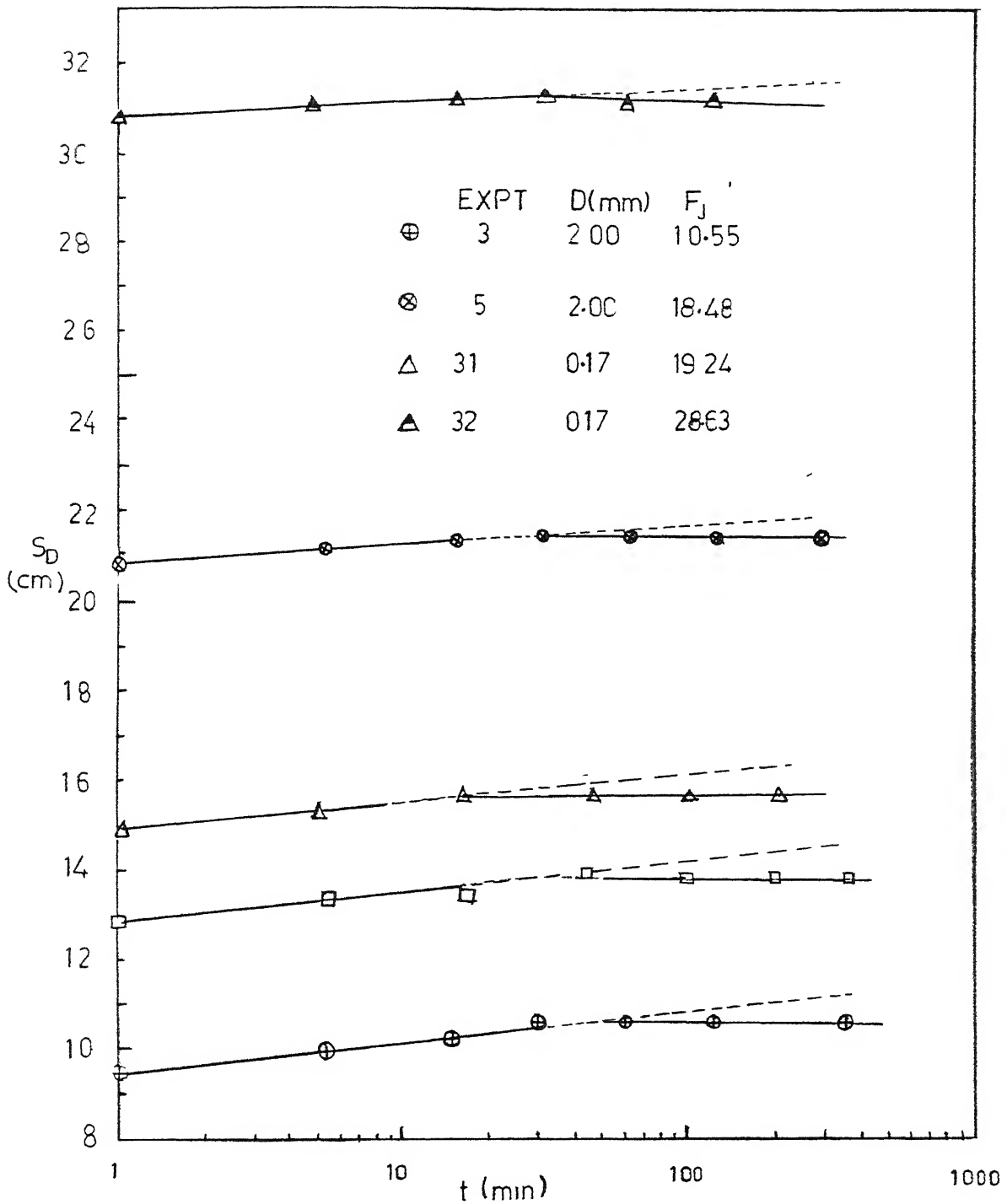


FIG. 5.3 INCREASE IN DYNAMIC SCOUR DEPTH (S_D) WITH TIME (t)

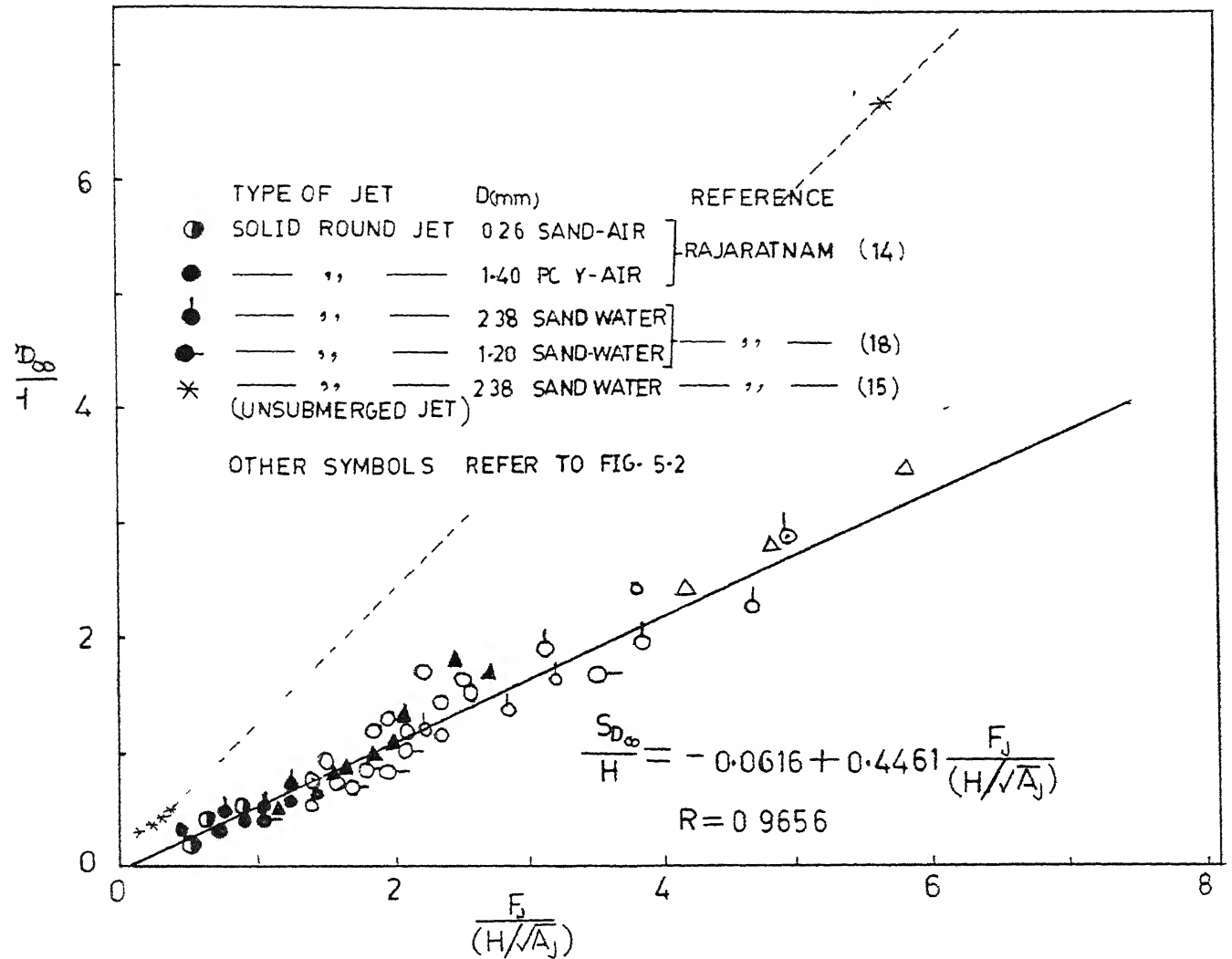


FIG 5.4 DYNAMIC SCOUR DEPTH AS A FUNCTION OF F_j

Acc No. A.1076

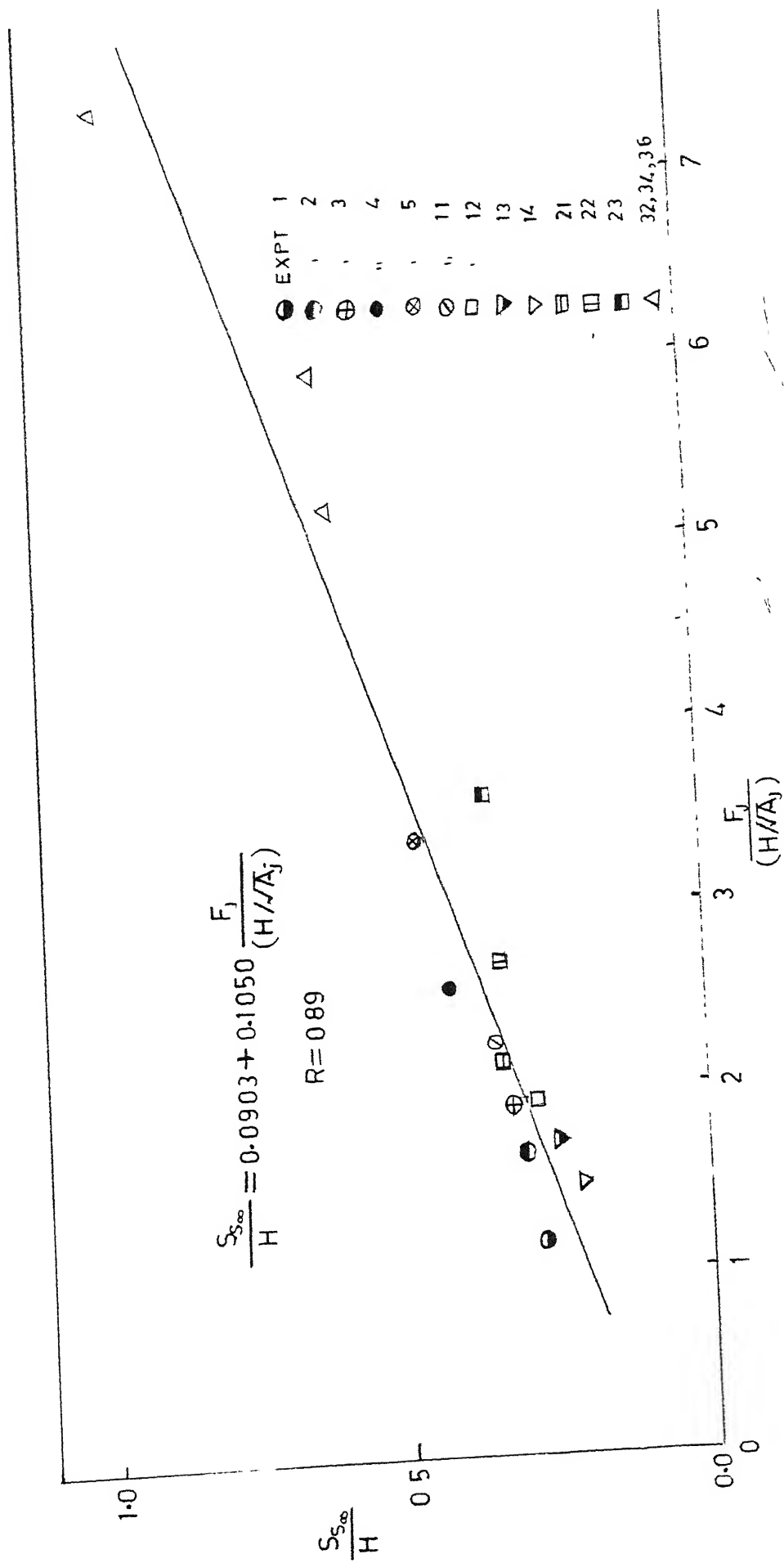


FIG 5.5 STATIC SCOUR DEPTH $S_{s\infty}$ AS A FUNCTION OF F_j

$$\frac{S_{S_{\infty}}}{H} = f_4 \left[\frac{F_j}{(H/\sqrt{A_j})} \right] \dots \dots \dots (5.9)$$

Fig. 5.5 shows the variation of nondimensionalised $S_{S_{\infty}}$ with $F_j/(H/\sqrt{A_j})$. The mean line shown in Fig. 5.5 can be represented by the equation

$$\frac{S_{S_{\infty}}}{H} = 0.0903 + 0.1050 \frac{F_j}{(H/\sqrt{A_j})} \dots \dots (5.10)$$

$R = 0.89$

5.2.3 Radius of Scour Hole

The radius of scour hole $r_{o_{\infty}}$ at original bed level, nondimensionalised by the depth of impingement H , with corresponding $F_j/(H/\sqrt{A_j})$ has been plotted in Fig. 5.6(a). This figure shows that the data points for 2.0 mm sand and 0.17 mm sand follow two different trends. This indicates the presence of some other forces which affect the scour process near the top of the scour hole. When the jet is started, it penetrates into the sand bed by eroding bed material. After a certain depth, when the scouring capacity of jet ceases, it deflects back and reaches the top of the scour hole with considerably smaller velocity. Since the velocity of undeflected jet remains very high, viscosity does not play a significant role but as the velocity of deflected jet becomes very small near the top of the scour hole, the effect of viscosity should be taken into consideration. For testing this, the values of $r_{o_{\infty}}/H$ are plotted with corresponding values of $F_j/P_1(H/\sqrt{A_j})$ in Fig. 5.6(b).

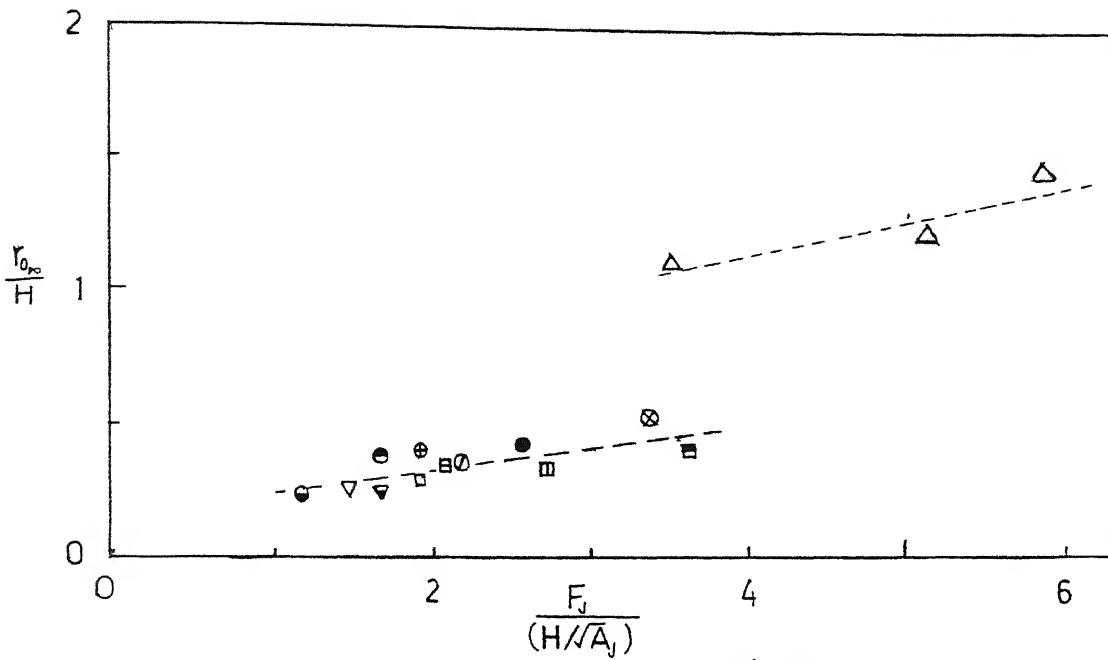


FIG 5 6(a) VARIATION OF $\frac{r_{\infty}}{H}$ WITH $\frac{F_J}{(H/\sqrt{A_J})}$

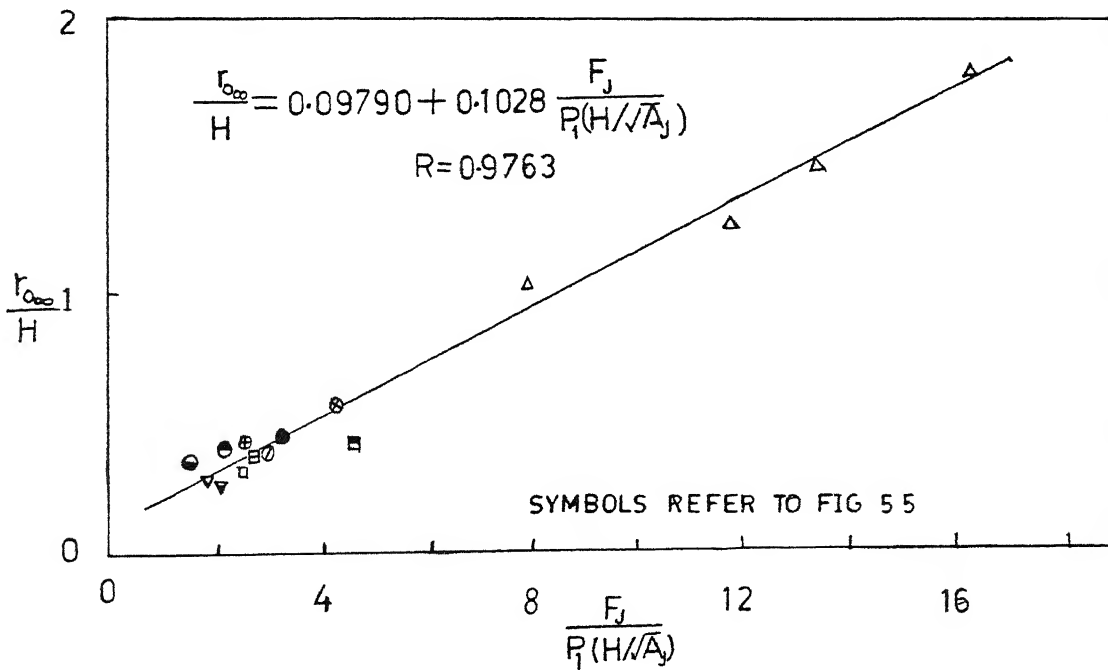


FIG 5 6(b) VARIATION OF $\frac{r_{\infty}}{H}$ WITH $\frac{F_J}{P_1(H/\sqrt{A_J})}$

$$\text{where } P_1 = \sqrt{(2/3) + \frac{36 \nu^2}{g D^3 \frac{\Delta P}{P}}} - \sqrt{\frac{36 \nu^2}{g D^3 \frac{\Delta P}{P}}} \dots \dots \dots (5.11)$$

(Ref.24)

and ν = kinematic viscosity of water.

Fig. 5.6 (b) shows that $r_{o\infty}/H$ varies linearly with $F_j/P_1(H/\sqrt{A_j})$ for both 2.0 mm and 0.17 mm sands and this variation is described by the equation

$$\frac{r_{o\infty}}{H} = 0.0979 + 0.1028 \frac{F_j}{P_1(H/\sqrt{A_j})} \dots \dots (5.12)$$

$R = 0.9763$

5.2.4 Scour Hole Profiles

During the study, it was observed that the eroded bed profiles for the different experiments appeared to be similar and hence the profiles were tested for similarity by plotting the $S_D/S_{D\infty}$ against r/r_x in which $S_{D\infty}$ is the depth of erosion at center (under the jet) and r_x = the length scale defined as the value of r in which $S_D = 0.5 S_{D\infty}$. Fig. 5.7 shows the dimensionless dynamic scour hole profiles for 2.00 mm sand. There is some scatter in the data points but it can be noticed that profiles are similar. Fig. 5.8 (a) shows some scour profiles in static condition, i.e. after stopping the jet. Dimensionless static scour profiles for 2.00 mm sand, are shown in Fig. 5.8(b). Fig. 5.9 and Fig. 5.10 show the scour profiles in dynamic and static conditions respectively, for 0.17 mm sand.

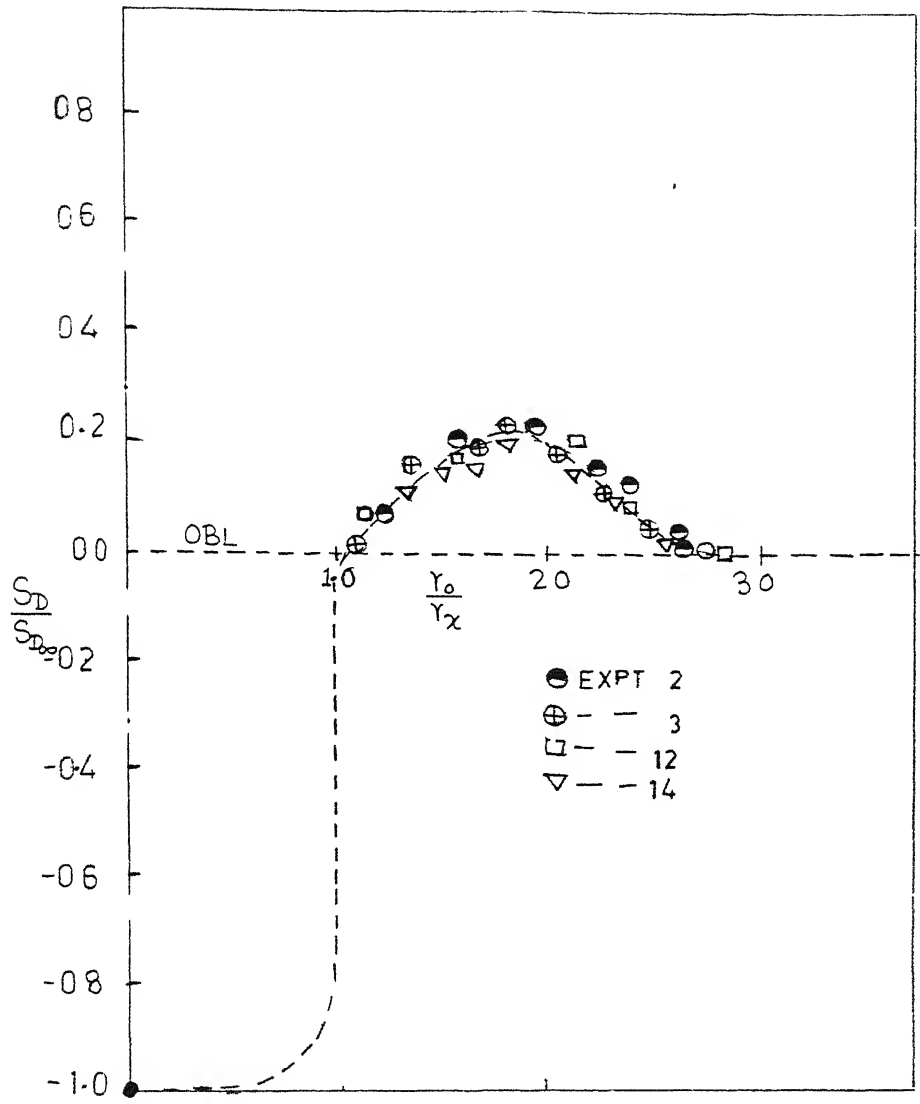


FIG 5.7 SIMILARITY OF DYNAMIC SCOUR PROFILES

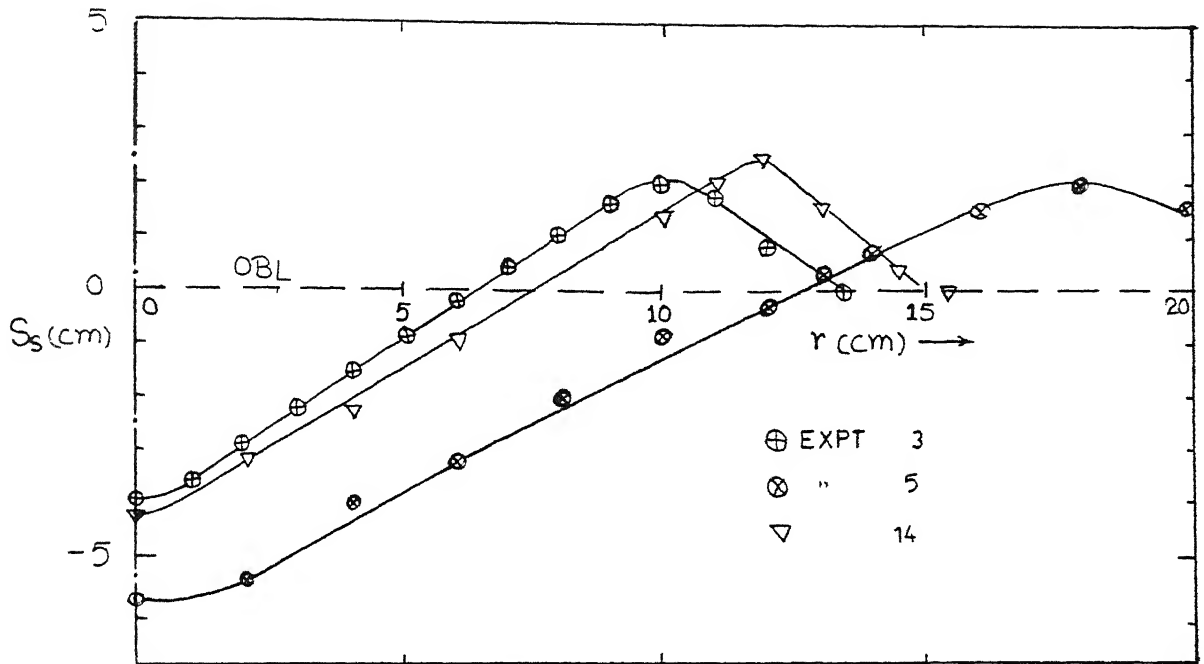


FIG. 5.8 ASYMPTOTIC ERODED BED PROFILES (STATIC)

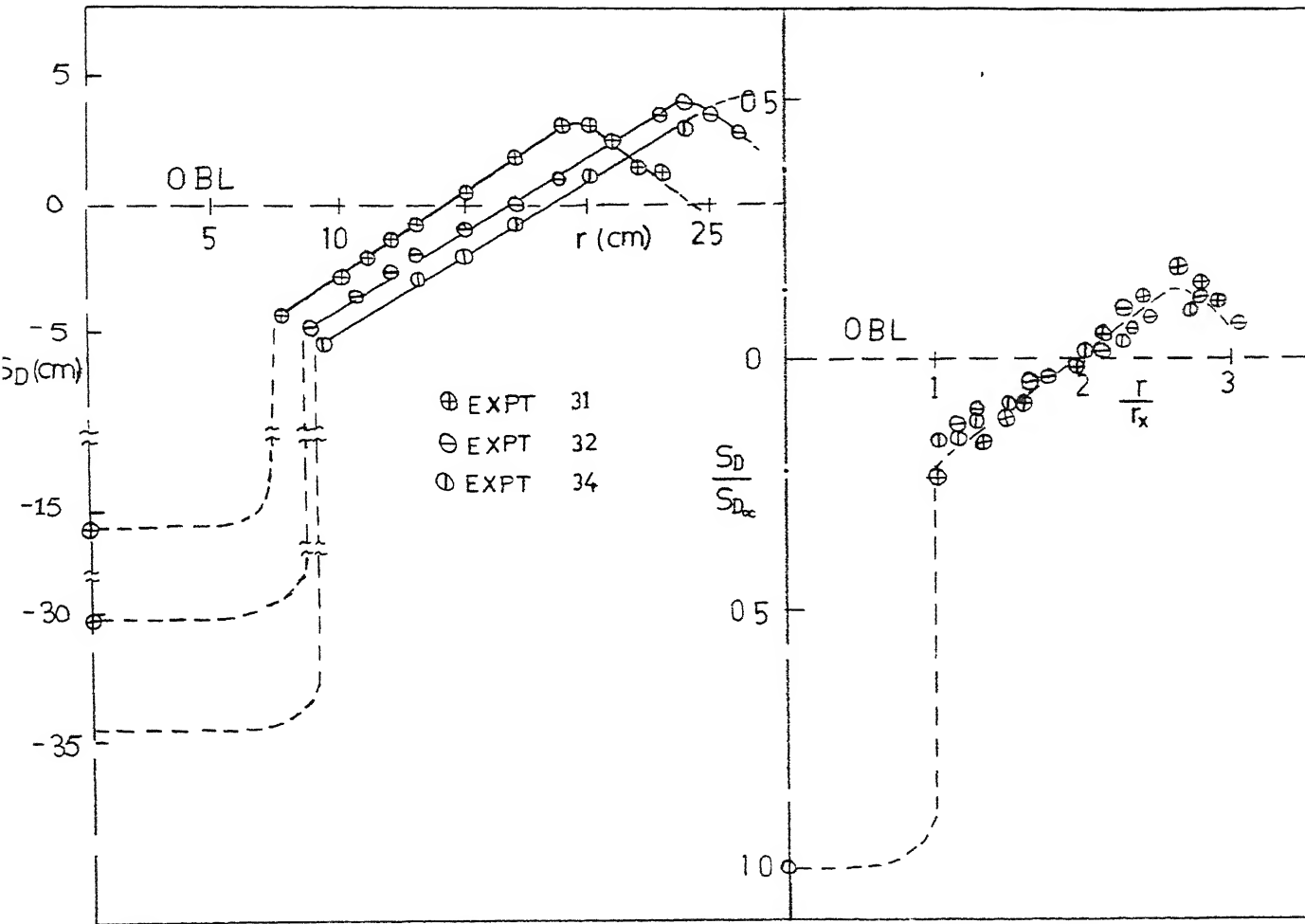


FIG 5.9(a) DYNAMIC SCOUR PROFILES

FIG 5.9(b) SIMILARITY OF DYNAMIC PROFILES

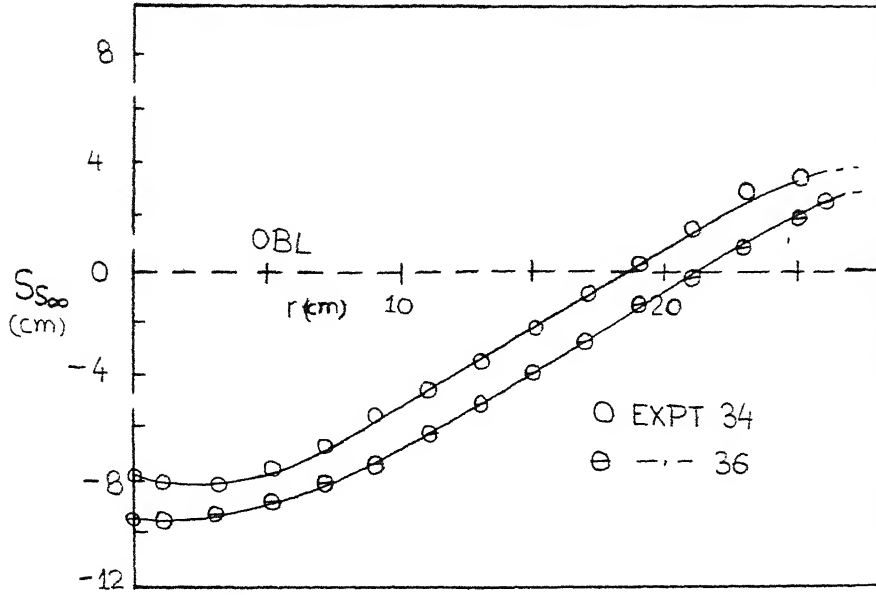


FIG 5 10(a) ASYMPTOTIC STATE ERODED
BED PROFILES (STATIC)

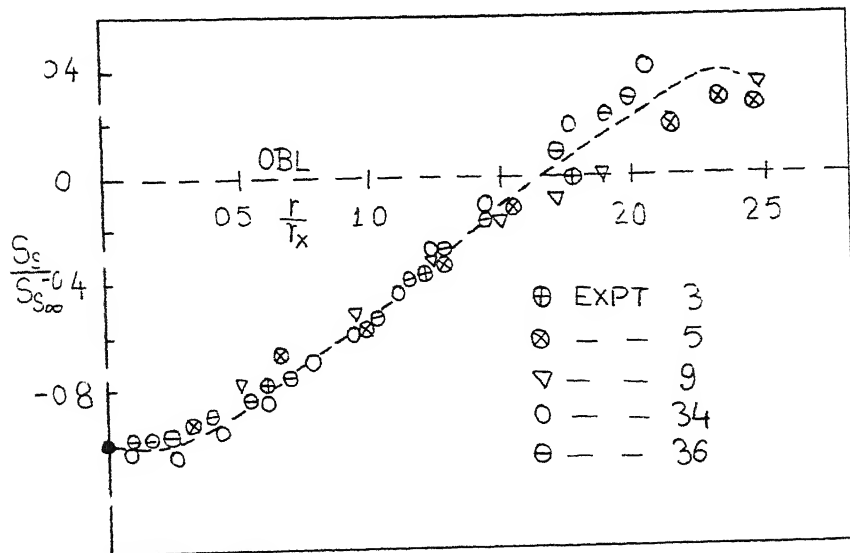


FIG 5 10(b) SIMILARITY OF STATIC SCOUR
PROFILES

They also show the similarity in the scour profiles. All these dynamic state profiles are described by a vertical face throughout most of the scour hole, followed by a slopping surface at the upper part with a ridge down stream of the bed. When the jet is stopped, the material in suspension and from up stream of the ridge settles quickly to fill part of the scour hole, with outward shift of the ridge. Bed slope, upstream and down stream of the ridge is equal to the angle of repose of the bed material.

5.3 Performance of Geotextiles

Details of geotextiles are given in Chapter 3. Some of the geotextiles are tested here as scour protection device. Geotextiles were placed at different elevations with respect to the sand bed level, in different test runs with constant submergence level H , and constant jet velocity U_j . Depression of geotextiles with time was noted. Figure 5.11 shows the increase in the Central depression of different geotextiles at different position for different runs with time. Figure 5.11 shows that for high velocity ($U_j = 4.62$ m/sec.), the geotextile assembly fails when it is placed at the bed level but does not fail when it is placed below bed level.

It was observed that when there was depression in the central part of the geotextile, i.e. below jet, the outer peripheral portion of the geotextile was heaved (Fig. 5.13) and the

anchors in that region tried to come out from sand bed. That was caused by the upward thrust exerted by water that had entered into the sand bed due to the force of the jet and deposition of bed material that had been removed from central portion. With higher jet velocity ($U_j = 4.61$ m/sec.) and when geotextile was placed at the sand bed level, piping below geotextile was effected by the seeping water with rapid removal of bed material from below the geotextile. Due to the combined effect of impact of jet on the geotextile and removal of material, the central portion of the geotextile was depressed into the bed and it got warped with failure of anchors. This state is considered as failure. One typical failure is shown in figure 5.12. This surface profile indicates the maximum depression at the centre of the geotextiles with steep downward slope near and towards the centre and increase in bed elevation in outer peripheral region.

No failure was observed when the geotextiles were placed below bed level, for same jet velocity ($U_j = 4.61$ m/sec.). During the experiments with geotextile placed below bed level, the outer peripheral portion of geotextile remain covered by bed material. Because of the presence of bed material above the geotextile, the failure was prevented. Its cause can be explained by the necessity of using filters on the down stream side of the dams and canal embankments.

For comparison, the dynamic surface profiles are shown in figure 5.13 with and without geotextile for same U_j and impingement height H . This figure shows the formation of deep cylindrical scour hole in sand bed without geotextile, but shows very small depression in central portion of the bed covered with geotextile and slight increase in bed elevation in outer region.

5.4 Comparison with Previous Work

Experimental data of air jet on sand bed and polystyrene, water jet on sand bed by Rajaratnam (1977, 1982) and data of circular wall jet of water on sand bed by Dwivedi (1988) are plotted in Figure 5.4, they follow the same trend for submerged case. Experimental data for unsubmerged case of sand water by Rajaratnam (1981) lie well above the data for submerged case. This shows that for the same grain size, the dynamic depth of scour in unsubmerged case is more than that for submerged case.

:::::

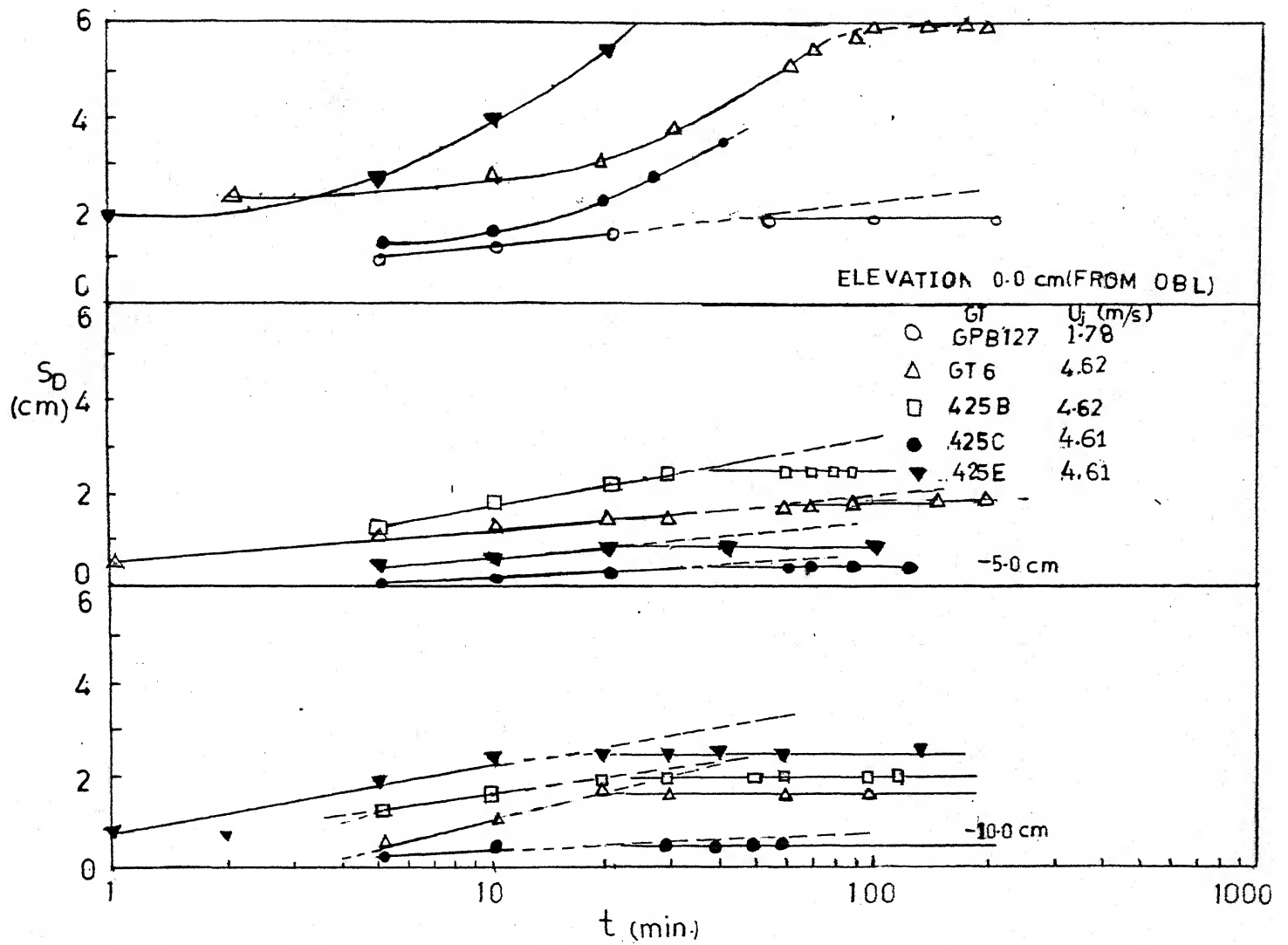


FIG 5.11 INCREASE IN DEPRESSION OF GEOTEXTILE WITH TIME

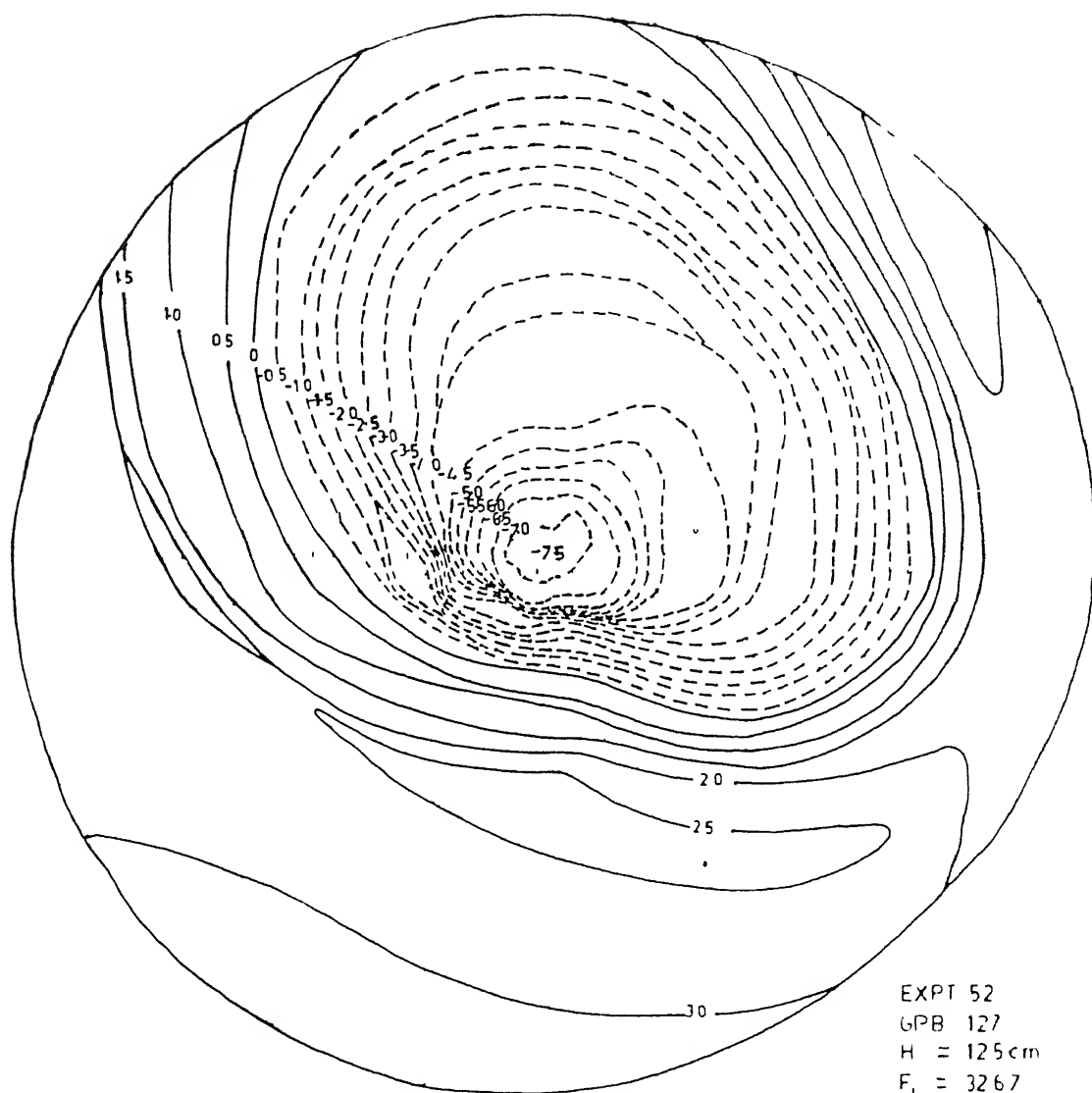


FIG. 512 BED PROFILE (STATIC) AFTER FAILURE OF GEOTEXTILE

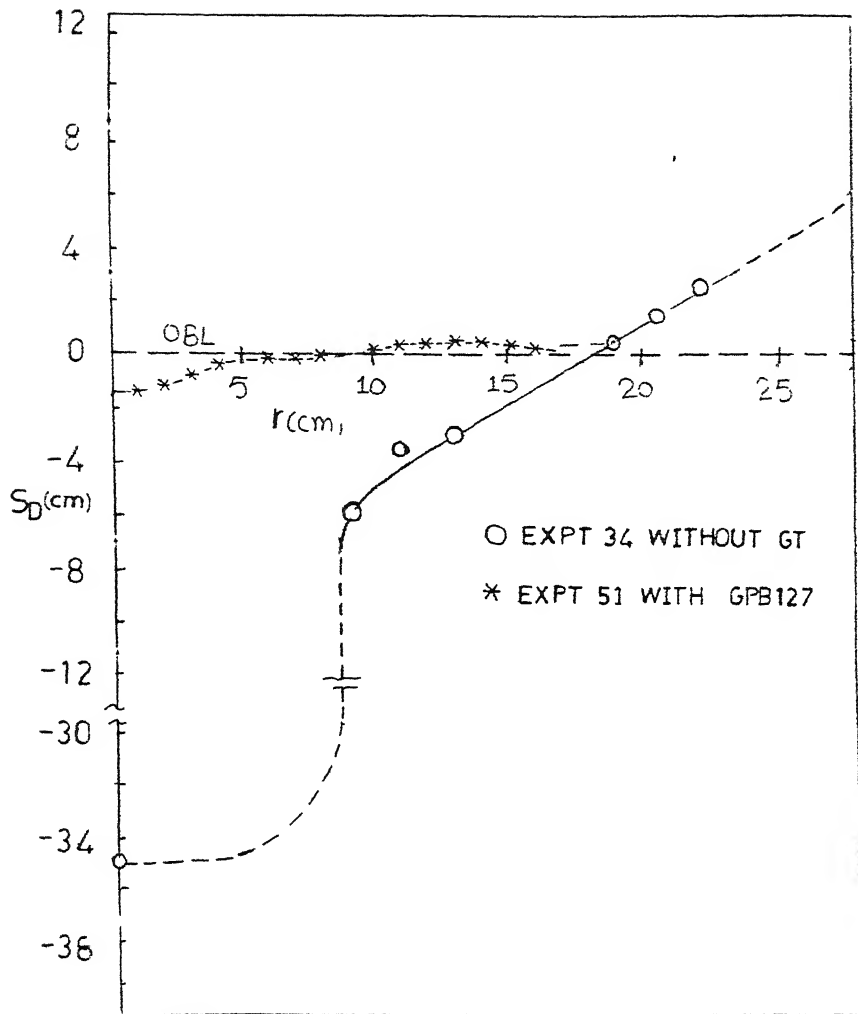


FIG 5.13 DYNAMIC BED PROFILES WITH
AND WITHOUT GEOTEXTILE

CHAPTER 6

CONCLUSIONS AND RECOMMENDATIONS

6.1 Conclusions

Based on an experimental study of the erosion of cohesionless sand beds by submerged impinging circular water jet and performance of geotextiles as scour protection measure, the following conclusions can be made. The axial velocity of jet decays linearly in axial direction in developed flow region. The maximum depth of dynamic erosion, occurring under jet, increases linearly with logarithm of time for a large part of the erosion process; then growth of this scour depth departs from the above mentioned relation to eventually reach an asymptotic or end state, the profile of the scour hole has been found to be similar. The asymptotic value of dynamic scour as well as static scour in terms of H have been found to be mainly functions of $F_j/(H/\sqrt{A_j})$. The asymptotic radius of scour hole (r_{oe}) in terms of depth of impingement H is a function of $F_j/P_1(H/\sqrt{A_j})$ where P_1 is a coefficient whose value depends on viscosity of fluid, median size and density of bed material. It is interesting to find that the present analysis

appears to be able to correlate reasonably well, the sand-air, polystyrene-water data, for circular solid jet, of Rajaratnam and sand water data, for annular wall jet of Dwivedi.

For scour protection, geotextiles can be used effectively. The geotextile assembly fails only due to failure of anchors and by removal of very fine sand particles from below the bed. Since geotextiles are flexible, permeable but have very fine pores, they can be used, with proper weighing down arrangement and anchorage, as scour protection measure without danger of bursting due to uplift pressure or removal of bed material.

6.2 Recommendation for Future Work

In present study, the bed/^{of} uniformly graded sands have been used. The armour action, the paving of coarse gravel at scoured surface occurs in bed material having a wide gradation, which generally occurs in practice and affects the scouring phenomena. Hence sediment of non-uniform bed of wide gradation should be used.

Container of large size should be used so that the area affected by jet can be found out. The jet should not be connected to the main overhead tank directly, it should be connected to a separate overhead tank with arrangement to deliver

water at constant head to eliminate the vibrations and velocity fluctuation.

Since the failure of geotextile assembly occurred due to failure of U-pin anchors, different type of anchorage arrangements should be used to keep the geotextiles in stretched condition. Sand and gravel of different grading should be placed below the geotextile and their effect on piping phenomenon and performance of geotextile should also be tested.

:::::

REFERENCES

1. Albertson, M.L., Dai, Y.B., Jensen, R.A. and Rouse, H. (1950) 'Diffusion of submerged Jets', Transactions, ASCE, Vol. 115 Paper No. 2409, pp. 639-664.
2. Beltaos, S. and Rajaratnam, N. (1973). 'Plane Turbulent Impinging Jets', J. of Hyd. Res. IAHR., Vol. 11, No.1, pp. 29-59.
3. Beltaos, S. and Rajaratnam, N. (1974). 'Impinging Circular Turbulent Jets', Proceedings, J. of Hyd. Div., ASCE. Vol.100, No. HY10, pp. 1313-1328.
4. Carsten, M.R. (1966), 'Similarity Laws for Localised Scour', J. of Hyd. Div., ASCE. Vol. 92, No. Hy3. p. 13.
5. Chatterjee, S.S. and Ghosh, S.N., (1980). 'Submerged Horizontal Jet Over Erodible Bed', J. of Hyd. Div., ASCE. Vol. 106, No. HY11. pp. 1675-1781.
6. Clarke, F.R.W. (1961), 'Report of M.Sc. Thesis. J. of Hyd. Res. IAHR. Vol. 13, pp. 160.
7. Doddiah, D., Alberston, M.L. and Thomas, R.A. (1953), 'Scour from Jets', Minnesota International Hydraulic Convention.
8. Dwivedi, V.K. (1988). 'Scour by Submerged Cylindrical Turbulent Impinging Wall Jets', M. Tech. Thesis, Department of Civil Engineering, I.I.T. Kanpur.

9. Godbole, M.L., and Mehendale, P.B. (1989), 'Scour Estimation and Protection for Road Bridge Across Tapi River Idgaon, Maharashtra'. Proc. of Third International Workshop on Alluvia River Problems, University of Roorkee, Roorkee.
10. Govind Rao, N.S. and Sarma, K.V.N. (1967). 'Scour Function'. J. of the Instt. of Engrs. (India). Vol. 47, No.5, CI 3, pp. 260-286.
11. John, A.W.M., 'Geotextiles', Published by Chapman and Hall, New York.
12. Loursen, E.M., (1952), 'Observation on the Nature of Scour'. Proc. of Fifth Hyd. Conference, Iowa State University Engineering Bulletin.
13. Rajaratnam, N. (1976), 'Turbulent Jets'. Development in Water Sciences, Elsevier Publ. Co., Amsterdam, Holland.
14. Rajaratnam, N. Beltaoss, S. (1977), 'Erosion by Impinging Circular Turbulent Jets'. Proceedings, ASCE. J. of Hyd. Div. Vol. 103, No. HY10, pp. 1191-1205.
15. Rajaratnam, N. (1981), 'Erosion of Sand Beds by Circular Impinging Water Jets with Minimum Tail Water Technical Report. Water Resources Engineering Group, Department of Civil Engineering, University of Alberta Edmonton, Canada.
16. Rajaratnam, N. (1981). 'Erosion by Plane Turbulent Jets'. J. of Hyd. Res., IAHR. No.4, pp. 339-358.

17. Rajaratnam, N., Pochylka, D.S. and Macdougall, R.K. (1981). 'Further Studies on the Erosion of Sand Beds by Plane Water Jets'. Water Resources Engineering Rept. WRE 81, Department of Civil Engineering, University of Alberta, Edmonton, Alberta, Canada.
18. Rajaratnam, N. (1982). 'Erosion by Submerged Circular Jets'. J. of Hyd. Engg., ASCE. Vol. 108, No. HY2. pp. 262-267.
19. Roerner, R.M., 'Durability and Aging of Geosynthetics'. Elsevier Applied Sciences, London and New York.
20. Hense, H., (1940), 'Criteria for Similarity in the Transportation of Sediment. Proceedings 1st Hydraulic Conference Bulletin 20, University of Iowa, Iowa, pp. 33-49.
21. Sarma, K.V.N., (1967), 'Existence of Limiting Scour Depth'. J. of Instt. of Engineers (India)., Vol. 48, No.1, CT.1. pp. 84-92.
22. Sarma, K.V.N. and Sivasankar, R. (1967), 'Scour Under Vertical Circular Jet'. J. of Instt. of Engineers (India), Vol. 48, No.3, CT2, p. 568-579.
23. Walter C. Mihand Kabir, J. (1983), 'Impingement of Water Jets on Non-uniform Stream bed'. J. of Hyd. Engineering, Vol. 109, No.4, pp. 536-548.
24. Vanoni, V.A. (Editor), (1977), 'Sedimentation Engineering, ASCE- Manuals and Reports on Engineering Practice No.54.